ECB 5034

FINAL YEAR RESEARCH PROJECT

DEVELOPMENT OF MODEL FOR REMOVAL OF CARBON DIOXIDE AND HYDROGEN SULFIDE FROM NATURAL GAS USING γ-ALUMINA MEMBRANE

By

RABIATUL FARAH MOHD LOTFI

Dissertation submitted in partial fulfilment of

the requirements for the

Bachelor of Engineering (Hons)

(Chemical Engineering)

JULY 2005

Universiti Teknologi PETRONAS

Bandar Seri Iskandar

31750 Tronoh

Perak

CERTIFICATION OF APPROVAL

DEVELOPMENT OF MODEL FOR REMOVAL OF CARBON DIOXIDE AND HYDROGEN SULFIDE FROM NATURAL GAS USING γ-ALUMINA MEMBRANE

BY

RABIATUL FARAH MOHD LOTFI

A project dissertation submitted to the
Chemical Engineering Programme
Universiti Teknologi PETRONAS
In partial fulfilment of the requirement for the
BARCHELOR OF ENGINEERING (Hons)
(CHEMICAL ENGINEERING)

APPROVED BY,

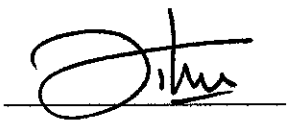

(DR HILMI MUKHTAR)
DATE: 29/7/05

UNIVERSITI TEKNOLOGI PETRONAS
TRONOH PERAK
JULY 2005

CERTIFICATION OF ORIGINALITY

This is to certify that I am responsible for the work submitted in this project, that the original work is my own except as specified in the references and acknowledgements, and that the original work contain herein have not been undertaken by unspecified source of persons.

_____

RABIATUL FARAH MOHD LOTFI

DATE:

EXECUTIVE SUMMARY

High operating cost all allocated for the removal of carbon dioxide and hydrogen sulphide from natural gas. The presence of these gases cannot be tolerated because they will cause major trouble in the gas processing system. Natural gas should be down to pipeline quality since these acidic gases are highly corrosive especially when of water moisture is presence in the stream. Also, Carbon dioxide does not contribute to the calorific value of natural gas. Membrane technologies have been commercially used in natural gas purification due to the proven advantages over other conventional methods. In order to achieve a good separation of gas components, membrane should acquire high selectivity and high permeability.

The main objective of this study is to develop a mathematical model to predict the removal of carbon dioxide and hydrogen sulfide from natural gas using γ-alumina membrane in pure mixed condition. The developed model is systematically analyzed to determine the factors that contributed to effective membrane separation such as pressure and pore size. The developed model describes the effect of mass transfer due to the pore diffusion (Knudsen and bulk diffusion), viscous diffusion and surface diffusion. Generally, the modelling results show the permeability of hydrogen sulfide is the highest followed by carbon dioxide and methane respectively. The permeability of binary mixture of CO_2/CH_4, H_2S/CH_4 and CO_2/H_2S depends on combination of gases in the mixture. Basically the permeability of faster gas will decrease with the addition of slow gas. On the contrary, the permeability of slow gas is predicted to be improved due to the combination with fast gas. The same trend is observed for the permeability gas in tertiary mixture. The model also shows that permeability of hydrogen sulphide increases as the pressure increased. However, the permeability of carbon dioxide and methane is independent of pressure.

ACKNOWLEDGEMENT

Foremost, I would like to express my deepest gratitude to Dr Hilmi Mukhtar for his supervision and guidance throughout this project. I truly appreciated his effort in providing constructive idea and advice toward the success of the project. His great support and assistance have enabled me to complete the project within the given time frame and achieve the project's objectives.

I would like to compliment the Department of Chemical Engineering of Universiti Teknologi PETRONAS for allocating such a good opportunity for us to be involved in research project. This is a very good platform to develop our creativity in order to be well rounded students. With this opportunity, we are able to sharpen our knowledge as well as developing our critical and analytical skill while interpreting the data.

Thanks to my colleague, Che Wan Azwa for sharing his idea and knowledge especially during modelling stage using Mathcad. Our discussion throughout the project has given major contribution to the success of the project.

Lastly but not the least, I would like to credit my family, friends and those who has directly or indirectly involved in this project, for their tremendous support and motivation.

TABLE OF CONTENTS

LIST OF FIGURES & TABLES

LIST OF FIGURES

LIST OF TABLES

NOMENCLATURE

M_i	Molecular weight	[g.mol^{-1}]
P'	Permeability	[mol.s.kg^{-1}]
P	Pressure	[bar]
T	Temperature	[K]
P_c	Critical Pressure	[bar]
T_c	Critical Temperature	[K]
r_p	pore radius	[m]
r	radius of gas molecule	[m]
t_m	membrane thickness	[m]
ρ_m	membrane density	[kg.m^{-3}]
τ	Tortuosity	[-]
ε	Porosity	[-]
z_i	compressibility factor	[-]
Ω_i	Lennard Jones potential	[-]
σ_i	Lennard Jones parameter	[Å]
ΔH_{adsi}	heat of adsorption	[kJ.kmol^{-1}]
x_i	mol fraction of species i	[-]
D_s	surface diffusivity	[m^2.s^{-1}]
D_k	Knudsen diffusivity	[m^2.s^{-1}]
D_{ij}	normal diffusion of species i into species j	[m^2.s^{-2}]
h	the uptake of gas species	[mol.kg^{-1}]
f	equilibrium loading factor	[m^3.kg^{-1}]
Cs	surface concentration	[mol.m^{-3}]
C	gas concentration	[mol.m^{-3}]
R	universal gas constant	[atm.m^3.mol^{-1}.K^{-1}]
μ	viscosity	[Pa.s]
μ_{mix}	viscosity of gas mixture	[Pa.s]

CHAPTER 1
INTRODUCTION

1.1 Background of Study

In this modernization era, the natural gas demand increases rapidly, corresponding to the innovation of new exploration and utilization technologies. According to a study conducted by Baker (2001), the total worldwide production of natural gas is about 50 trillion standard cubic feet per year. Currently, Malaysia produces approximately 2 billion standard cubic feet per day (Ng et al, 2004). This indicates the significant of natural gas production as a substantial part in Malaysian economic development.

1.1.2 Natural Gas

Natural gas is formed from sediments that are rich in organics matter which have been treated at very high temperature and pressure in the underground reservoir for millions of years. It is chemically interpreted as the composition of primarily methane with smaller amounts of other hydrocarbons, nitrogen, carbon dioxide, hydrogen sulfide and other impurities. According to Hyne (2001) these gaseous impurities are called inert because they do not 'burn' in natural gas.

Natural gas exists in the gaseous form or mixture with natural crude oil. Natural gas is classified into 2; associated and non-associated natural gas (Matar and Hatch, 2001). Non-associated gas is found in the dry well which contains no oil. While associated gas dissolves in crude oil and is found intermingling in the reservoir.

The composition of natural gas is unique and varies accordingly from one reservoir to another. The following is the table outlining the typical make up of natural gas. The table states clearly the composition of hydrogen sulfide and carbon dioxide from different locations in the world. In some countries, like Saudi Arabia, the existence of hydrogen sulfide and carbon dioxide are very high. On the hand, there is only a negligible amount of sour component in Kliffside, United States.

Table 1.1 Composition of non-associated and associated natural gas (Matar and Hatch, 2001)

	Non-associated gas		**Associated gas**	
Component	**Salt Lake US**	**Kliffside US**	**Abqaiq Saudi Arabia**	**North Sea UK**
Methane	95.0	65.8	62.2	85.9
Ethane	0.8	3.8	15.1	8.1
Propane	0.2	1.7	6.6	2.7
Butane	-	0.8	2.4	0..9
Pentane and heavier	-	0.5	1.1	0.3
Hydrogen Sulfide	-	-	2.8	-
Carbon dioxide	3.6	-	9.2	1.6
Nitrogen	0.4	25.6	-	0.5
Helium	-	1.8	-	-

The composition of the gas delivered to the pipeline is tightly controlled. Therefore, removal of acid gas components such as carbon dioxide and hydrogen sulfide are very crucial operation in natural gas processing industry. With the increase demand for natural gas as the energy of choice in many applications, the purification or acid gas sweetening process to a pipeline or cryogenic quality (Yunus and Radhakrishnan, 2004) has turned out to be the foremost issue in the exploitation and utilization of natural gas. Table 1.2 shows the natural gas specification that should be achieved before being

exported to United States. The specification is assumed to be the same all over the world.

Table 1.2: Composition Specification for Natural Gas delivery to US National Pipeline Grid (Baker, 2001)

Component	Specification
Carbon Dioxide	< 2%
Water	< 120 ppm
Hydrogen Sulfide	< 4 ppm
Propane and heavier	950 – 1050
Total inert gas	< 4%

However, in a study done by Carnell and Towler (1997), they highlighted to lower the hydrogen sulfide pipeline specification to 1 ppm after discovering the link between hydrogen sulfide concentration and the failure of gas metering as well as supply equipment.

1.1.2 Natural Gas Treatment using Membrane

Gas treating technologies have been rapidly developed in order to remove the impurities to meet the required specifications. A wide variety of applications are currently available. They included absorption process, swing adsorption and membrane separation. Membrane technology is the most environment friendly alternative to substitute amine wash technology.

The advantages of membrane system over other conventional technology are summarizes as follows based on the study by Dortmundt and Doshi, 1999 and Baker, 2001.

- Lower capital cost because the system requires no solvent storage and water treatment as compared to traditional amine wash technology.

- Operational simplicity and high reliability because it has no moving part therefore low possibility of unscheduled downtime. The plant also does not require full time supervision and intensive labor.
- Good weight and efficiency. Space efficiency is crucial for offshore environment where deck area is restricted.
- Environmentally friendly since it does not involve periodic removal of solvent.
- Ideal for remote location where spare parts are rare, labor are unskilled and extensive infrastructure is unnecessary.

Due to these factors, it is a brilliant choice to adapt membrane technology in gas processing plant to remove acid gas impurities.

Gas dissolves and diffuses into membrane if a pressure differential is set up on opposing side of membrane. According to the principle, small molecules of CO_2 and H_2S permeate faster than large molecules such as N_2 and hydrocarbon. In membrane separation, acid gas is separated from natural gas mixture when the carbon dioxide and hydrogen sulfide passed through a nonporous membrane. Due to differences in their molecular size and solubility in the membrane polymer, acid gas has different membrane permeation rate from natural gas.

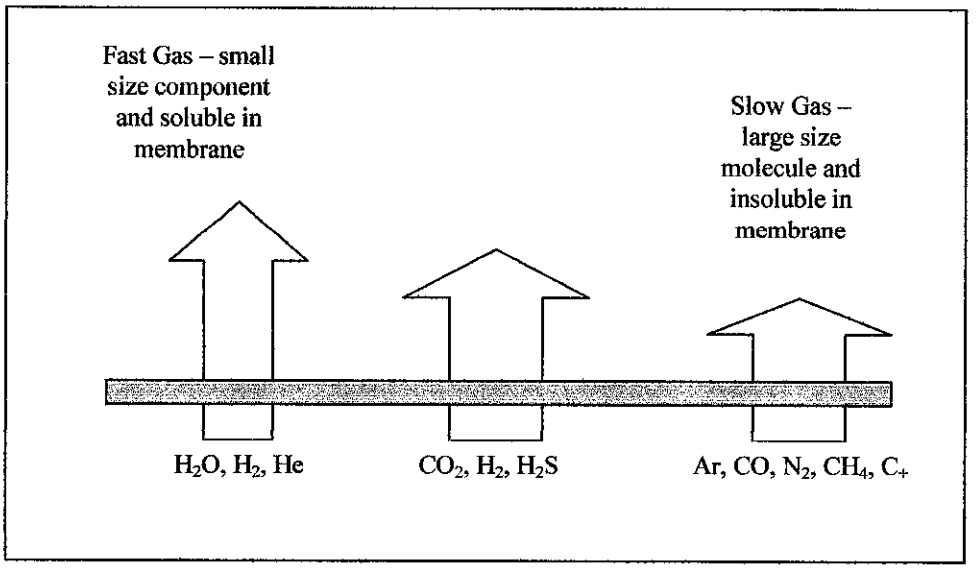

Figure 1.1 Typical classifications of fast and slow gases across membrane

Basically, molecular size and solubility of molecules are determined by their molecular geometry. Molecular geometry is the three-dimensional arrangement of atoms in a molecule which affects the physical and chemical properties of molecules. It can be divided into linear, trigonal planar, tetrahedral, bipyramidal and octahedral.

The slow movement of methane molecules is caused its complex tetrahedral structure. A tetrahedron has four sides of equilateral triangles. In a tetrahedral molecule, the central atom (carbon) is located at the center of the tetrahedron and the other 4 atoms are located at the corner with bond angel of 109.5°.

Both carbon dioxide and hydrogen sulfide are triatomic molecules, which have either linear or bent geometry. For a molecule made up of three or more atoms, the molecular geometry is strongly dependent of dipole moment. Two bond moments in carbon dioxide are equal in magnitude and the sum of resultant dipole moment is zero. Hence carbon dioxide is concluded to have linear molecular geometry. On the other hand, hydrogen sulfide has a bent molecular geometry because the two bond moment partially reinforced each other. Due to their structures, carbon dioxide and hydrogen sulfide moves smoothly across membrane.

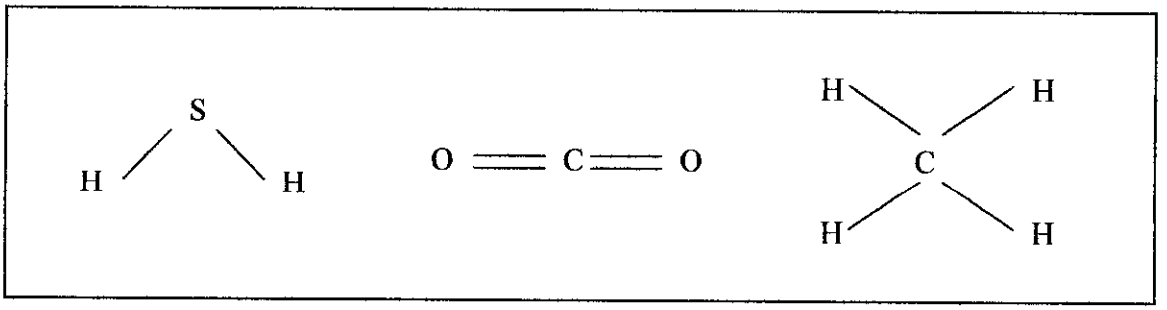

Figure 1.2 Molecular geometry of hydrogen sulfide, carbon dioxide and methane

Permeability and selectivity are two major considerations that must be taken into account to produce a good membrane separation process. However, in some cases, it is not industrially practical to applied membrane separation. For example is the separation of nitrogen from methane. Since a polymer membrane rarely has nitrogen/methane

selectivity greater than 2 (Coker et al, 2003), there will be a large loss of methane into permeable stream and little nitrogen removal of methane.

1.1.3 Development of Membrane Technology

Fundamental mechanism of gas transport across a polymer membrane was first described by Sir Thomas Graham more than a century ago (Coker et al, 2003). However, since 1980s (Li, 2000) membrane based gas absorption process have obtained a myriad of attention. During this modernization era, the development of advance membrane technology has growth rapidly in order to enhance the reliability and extend performance of membrane separation process. The impact of the developments is appreciably significant and is summarized in the following table.

Table 1.3: Milestones of the important development in membrane gas separation (Baker, 2001 and Baker et al, 2003)

Year	Achievement
1850 - 1949	• Development of Diffusion Law by Graham
1950 - 1959	• Development of first systematic permeability measurements by Van Amerongan Barrer
1960 - 1969	• Development of first anisotropic membrane in 1961 • Developed of spiral wound and hollow fiber modules for reverse osmosis
1970 - 1979	• -
1980 - 1989	• Introduction of Permea PRISM membrane in 1980 • Production of first N_2/Air separation system by Generon in 1982 • Development of advanced membrane material for O_2/N_2, H_2/N_2 and H_2/CH_4 separation

	launched by Ube, Medal, Generon in 1987 • Development and installation of first commercial vapor separation plants by MTR, GKSS, Nitto Denko in 1988 • Development of dried membrane for CO_2/CH_4 natural gas production by Separex, Cynara, GMS.
1990 - 1999	• Development of medal polyimide hollow fiber for CO_2/CH_4 separation installed in 1994 • Installation of first propylene/N_2 separation plants in 1996
2000 - now	• Development and installation of natural gas – nitrogen removal system by MTR in 2002

Membrane technologies have been commercially used in natural gas and petroleum refining industries due the proven advantages over other conventional method. For instance, UOP have installed more than 80 membranes units in various countries such as Pakistan, Taiwan, Mexico, Egypt and United States of America (Dortmundt and Doshi, 1999).

The key to an efficient and economical membrane separation process is good membrane permeability, high selectivity, stability and long life (more than 2 years). In order to achieve a good separation, the membrane selectivity of the desired components should be higher. On a research done by Baker (2001), membrane selectivity of carbon dioxide/methane for cellulose acetate is about 12 – 15 while the selectivity of polyimide and polyamaride membranes is 20 – 25. Recently, more study is still up going to improve and produce a membrane with selectivity of 40.

1.2 Problem Statement

1.2.1 Critical problem causes by carbon dioxide and hydrogen sulfide in natural gas

The presence of acid gas such as carbon dioxide and hydrogen sulfide in natural gas stream cannot be tolerated. Natural gas should be treated or purified to remove the unnecessary substances (carbon dioxide and hydrogen sulfide) down to pipeline quality (Hilmi and Lim, 2004).

Carbon dioxide is highly corrosive with the presence of water within transportation and storage system (Li et al, 2005). According to Dortmunndt and Doshi (1999), the corrosion can destroy pipelines and equipment unless an expensive construction material is applied.

Besides, carbon dioxide and hydrogen sulfide does not contribute to the calorific value of gas (Chan and Miskon, 2004). Theoretically, calorific value is the heat content per unit volume of natural gas and is typically measured in Btu per cubic feet. Calorific value of pipeline natural gas is range from 900 to 1200 Btu/ft^3 (Hyne, 2001). The heat content of natural gas varies with the hydrocarbon composition and the amount of inert such as carbon dioxide and hydrogen sulfide. Higher amount of carbon dioxide reduces the heating value of natural gas stream because it carries zero amount of heat.

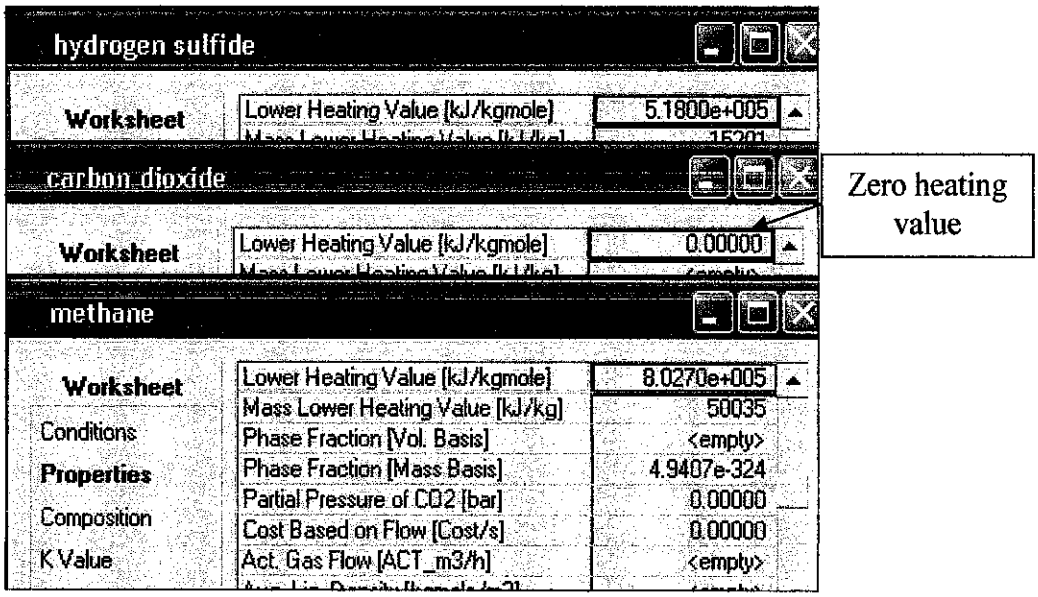

Figure 1.3: Amount of heating value simulated by Hysys

According to Chan and Miskon (2004), hydrogen sulfide has to be removed due to its toxic and acidic properties. K. Li et al (1998) also highlighted that hydrogen sulfide is one of the major sources that lead to the crucial environmental issue known as acid rain. The acidic feature of hydrogen sulfide contributes to the corrosiveness of pipeline and metallic equipment (Matar and Hatch, 2004)

1.2.1 Critical Problem in membrane separation process

This study will focus on the membrane separation technique of carbon dioxide and hydrogen sulfide from natural gas. Further research in membrane technology is significant, parallel with the robust development of the technology in variety of gas processing plants. One of the issue and constraint in membrane technology is the capacity. The application of existing commercial membrane separation technology is limited to small capacity up to 250 MMSCFD (Dortmudt and Doshi, 1999). Therefore is not suitable for throughput higher than that. However, the latest study by Li et al (2005), currently the largest capacity of membrane facilities for carbon dioxide removal is 700 MMSCFD.

Another limitation of membrane technology is high methane loss during natural gas purification unless a recycle stage is included (Carnell and Towler, 1997). Currently, most of membrane processes suffer about 20% (Hilmi and Lim, 2004) lost of methane. Therefore, in order to prevent this problem, it is suggested to apply multi-stage membrane to increase the methane recovery. However, there will be a lot more investment to install multi-stage system.

1.3 Objective and Scope of Study

The main objective of this study is (i) to develop a mathematical model to predict the removal of carbon dioxide and hydrogen sulfide from natural gas by γ alumina membrane and (ii) to analyze the factors that contributed to effective membrane separation such as pressure and pore size. The developed model describes the effect of mass transfer due to the pore diffusion (Knudsen and bulk diffusion), viscous flow and surface diffusion

Formerly studies of single component and binary system have been conducted. The initiatives of these studies have contributed to the extension of membrane technology. This study is significant because it deliberates on multiple or tertiary separation system, a step forward into the development of advance technology.

Generally, the study will focus on the following tasks:

1. Reproducing data of previous study
2. Permeability of pure component
3. Permeability of binary component
4. Permeability of ternary component

Based on the data of the tasks, interpretation will be done to compare the impact of binary and tertiary components system. Besides, this study will identify the dominate permeability effect of the model.

CHAPTER 2
LITERATURE REVIEW AND THEORY

2.1 Membrane Separation Mechanism

Membrane technology relies on the differences of the component permeation rates when they pass the membrane material. (Quinn et al, 2003). Due to the differences, the fast permeating species can be separated from slow permeating species.

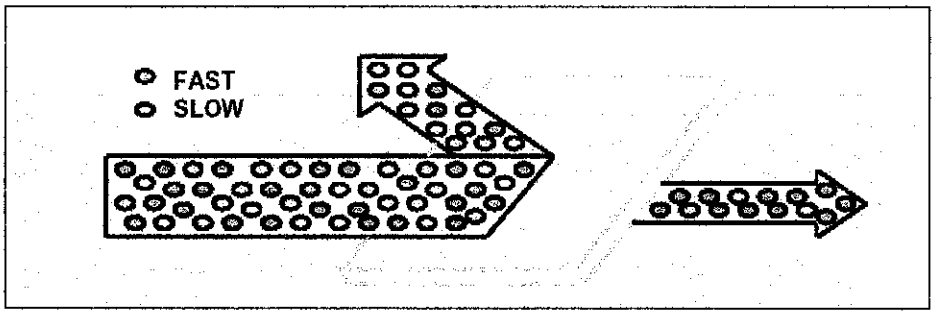

Figure 2.1: Permeation of gas component across membrane

In membrane process high pressure feed is supplied to one side of the membrane and permeate to the normal to the membrane. Typically, membrane separation consist of three compartment namely feed, retentate and permeate. Basically, the part of feed mixture that does not pass through the membrane is called retentate because it retains in the system. The component that pass through the membrane is called permeate.

2.2 Mass Transport across Membrane

Mass transport occurs when a component in a mixture migrates because of difference in concentration between two points. In principles, mass transport in porous particle is the result of four basic mechanisms.

- Bulk flow
- Molecular diffusion
- Knudsen diffusion
- Surface diffusion
- Viscous diffusion

2.2.1 Bulk flow

Bulk flow of a fluid happens due to the pressure difference through idealized straight cylindrical pores. In almost case, the flow is considered in the laminar regime when the pore diameter is very small. The flow velocity is given by Hagen-Poiseuille Law and is directly proportional to trans membrane pressure drop:

$$v = \frac{D^2}{32\mu L}\left(P_0 - P_L\right) \tag{2.1}$$

Where D is the pore diameter, μ is the viscosity and L is the length of pore. This law assumes that a parabolic velocity profile exists across the pore radius and the fluid is Newtonian.

Bulk diffusion is significantly important in large pores and at high pressures. Seader and Henly (1998) expressed the bulk flow permeability as follows:

$$P_{M_{bulk,i}} = \frac{\rho\varepsilon^3}{2(1-\varepsilon)^2 \tau a_v^{\,2} \mu} \tag{2.2}$$

2.2.3 Molecular diffusion

The diffusivity of binary gas in a dilute gas region at low pressure can be predicted using kinetic theory of gases. The gas is assumed to consist rigid spherical particles that are completely elastic on collision and the momentum is conserved. The equation of mean free path λor average distance of molecules without attractive and repulsive force is as follows:

$$D_{ij} = \frac{1}{3}\bar{u}\lambda \tag{2.3}$$

For a more accurate prediction of the gases kinetics, the intermolecular forces of attraction and repulsion between molecules should be taken into account. For non polar molecules, a reasonable approximation to the forces is Lennard Jones function.

$$D_{ij} = \frac{1.8583\times10^{-7}T^{3/2}}{P\sigma_{ij}^{2}\Omega_{D,ij}}\left(\frac{1}{M_i}+\frac{1}{M_j}\right)^{1/2} \tag{2.4}$$

Since the equation is relatively complicated to be used and some of the constant such as σ_{ij} are not available or difficult to estimate, it is more convenient to apply Fuller semi empirical method. The equation is obtained by correlating data with atomic volume of gas molecules.

$$D_{ij} = \frac{1.00\times10^{-7}T^{1.75}\left(1/M_i+1/M_j\right)^{1/2}}{P\left[\left(\sum v_i\right)^{1/3}+\left(\sum v_j\right)^{1/3}\right]^{3}} \tag{2.5}$$

Geankoplis (1993) suggested another method of determining molecular diffusion using simpler parameters which are the operating and critical conditions.

$$D_{ij} = a\left(\frac{T}{\sqrt{T_{ci}T_{cj}}}\right)^{b}\frac{\left(P_{ci}P_{cj}\right)^{1/3}}{P}\left(T_{ci}T_{cj}\right)^{5/12}\left(\frac{1}{M_i}+\frac{1}{M_j}\right)^{1/2} \tag{2.6}$$

Where a=2.745×10^{-4} and b= 1.823

For multi component mixture, the normal gas diffusion of component *i* in gases mixture is given as follows

$$D_{i,mix} = \frac{1}{\frac{x_j}{D_{ij}} + \frac{x_k}{D_{ik}} + .. + \frac{x_n}{D_{in}}} \tag{2.7}$$

Where *x* represents the mole fraction of each gas species.

2.2.3 Knudsen diffusion

Knudsen diffusion occurs due to the molecular-wall collision. It becomes dominant when the mean-free path, λ of the molecular species is much larger than the pores diameter.

Knudsen diffusion is independent of pressure and is calculated from

$$D_{k_i} = \frac{2}{3} r_p \bar{v}_i \tag{2.8}$$

Using the kinetic theory of gases to evaluate $\bar{v}_i$, the final equation for D_{k_i} if cylinder pores are assumed (Jareman et al, 2004) is as follows

$$D_{k_i} = 97 r_p \left(\frac{T}{M_i} \right)^{1/2} \tag{2.9}$$

$$D_{k,i} = \frac{2(r_p - r_i)}{3} \sqrt{\frac{8RT}{\pi M_i}} \tag{2.10}$$

For gas, diffusion may occur by ordinary diffusion in series with Knudsen diffusion when pore diameter is very small or total pressure is low. In Knudsen diffusion, the effect only occurs when the pore size is greater than the molecules size. In the Knudsen flow regime, collision occurs primarily between gas molecules and the pore walls rather than between gas molecules. Thus in the absence of bulk effect the gas flow equation is as follows:

$$D_{e_i} = \frac{\varepsilon}{\tau}\left[\frac{1}{(1/D_i)+(1/D_{k_i})}\right] \tag{2.11}$$

Therefore the permeability of gas diffusion can be expressed as below:

$$P_{M_{k,i}} = \frac{\varepsilon}{zRT\tau}\left[\frac{1}{(1/D_i)+(1/D_{k_i})}\right] \tag{2.12}$$

When the mean free path λ is small compared to the pore diameter d, molecule-molecule collision predominate and molecule-wall collision diminishes since the diffusion deviate from Knudsen type to Fickian type.

2.2.4 Viscous diffusion

Gas flow due to the pressure gradients is called viscous flow or Poiseuille flow. The viscous flow parameter B_o depends on the shape of the pores and can be calculated from Poiseulle flow relationship.

$$B_o = \frac{r_p^{\,2}}{8} \tag{2.13}$$

Mugge et al (2001) have developed the equation to describe total molar flux of viscous flow.

$$N_i^{viscous} = -\frac{p_i}{RT}\frac{B_o}{\eta}\frac{dP_{total}}{dz} \tag{2.14}$$

Hilmi Mukhtar and Lim Chin Han (2004) have expanded the viscous flow permeability as a function of membrane porosity pore size, tortuosity and viscosity as the following:

$$P_{M_{viscous,i}} = \frac{\varepsilon r_p^2 P}{8\tau\mu_i zRT} \tag{2.15}$$

The viscosity of a pure monatomic gas of molecular weight M may be written in term of Lennard-Jones parameters as

$$\mu = \frac{5}{16}\frac{\sqrt{\pi mKT}}{\pi\sigma^2\Omega_\mu} \tag{2.16}$$

or

$$\mu = 2.6693\times10^{-5}\frac{\sqrt{MT}}{\sigma^2\Omega_\mu} \tag{2.17}$$

In the second form of this equation, T [=] K and σ [=] Å and μ [=] g/cm.s. The dimensionless quantity Ω_μ is a slowly varying function of the dimensionless temperature $\kappa T/\varepsilon$, of the order of magnitude of unity given in table. It is called the collision integral for viscosity because it takes into account the details of the path taken by the molecules by binary collision. If the gas were made up of rigid spheres of diameter σ, then Ω_μ would be exactly unity. Hence the function of Ω_μ may be interpreted as describing the deviation from rigid sphere behavior.

2.2.5 Surface diffusion

Value of surface diffusivity of light gases for physical adsorption is typically in the range of $5\times10^{-3}-10^{-6}cm^2/s$ with the larger values applying to cases of a low differential heat of adsorption. For non polar adsorbates, the surface diffusivity in cm^2/s may be estimated from the following correlation

$$D_s = 1.6\times10^{-2}e\left[-0.45\left(-\Delta H_{ads}\right)/mRT\right] \tag{2.18}$$

Where m = 2 for conducting adsorbent such as carbon and m = 1 for insulating adsorbent. ΔH_{ads} is the specific enthalpy difference of adsorption of a species at specific temperature and pressure. A simple formula of estimating the heat of adsorption is applying the Trouton's Rule of heat of vaporization.

For non polar liquid

$$\Delta H_v(kJ/mol) = 0.088T_b(K) \tag{2.19}$$

For water, low molecular weight alcohol

$$\Delta H_v(kJ/mol) = 0.109T_b(K) \tag{2.20}$$

D_s value is then substituted in equation 2.17 which represents the surface permeability

$$P_{M_{surface,i}} = 2\frac{t_m\varepsilon}{r_p\tau}(1-\varepsilon)(D_s\rho_m f) \tag{2.21}$$

Equilibrium loading factor, f is approximated using Henry's constant which represent the solubility of gas. According to Hu et al (2003), gas permeation is dominated by diffusion of Henry's Mode. The correlation between f and the gases is obtained from equation

$$h = \frac{(fP)}{zRT} \tag{2.22}$$

whereby f increases with increasing temperature and decreasing temperature. h is the uptake of gas specie and is estimated using the equation

$$h = \frac{C_s}{\rho_m}. \tag{2.23}$$

The concentration at surface condition is assumed to be similar to the gas concentration, $C_s \approx C_1$ and is calculated using ideal gas correlation.

$$C = \frac{n}{V} = \frac{P}{zRT} \tag{2.24}$$

2.2.6 Total Permeability

Hilmi and Lim (2004) had extended the permeability correlation by summing up the individuals effect of diffusivity. The following equation indicates the correlation used for or pure component and gas mixture.

For pure component

$$P'_i = \frac{\varepsilon r_p^2 P}{8\tau\mu_i zRT} + \frac{\varepsilon}{z\tau RT}\left[\left(\frac{1}{1/D_i + 1/D_{k,i}}\right) + 2\frac{t_m\varepsilon}{r_p\tau}(1-\varepsilon)(D_s\rho_m f)\right] \tag{2.25}$$

For gases mixture

$$P'_{i,mix} = \frac{\varepsilon r_p^2 P}{8\tau\mu_{mix} zRT} + \frac{\varepsilon}{z\tau RT}\left[\left(\frac{1}{1/D_{i,mix} + 1/D_{k,i}}\right) + 2\frac{t_m\varepsilon}{r_p\tau}(1-\varepsilon)(D_s\rho_m f)\right] \tag{2.26}$$

There are two parameters that distinguish the permeability of gas mixture and pure component; viscosity and molecular diffusivity.

To calculate the viscosity of gas mixture μ_{mix} ,the multi component extension of Chapman-Enskog theory or semi empirical formula can be applied:

$$\mu_{mix} = \sum_{i=1}^{n}\left[\frac{x_i\mu_i}{\sum_j^n x_j\Phi_{ij}}\right] \tag{2.27}$$

where x_i is the mole ratio of species *i* in mixture. The dimensionless quantity Φ_{ij} is defined as:

$$\Phi_{ij} = \frac{1}{\sqrt{8}}\left(1+\frac{M_i}{M_j}\right)^{-1/2}\left[1+\left(\frac{\mu_i}{\mu_j}\right)^{1/2}\left(\frac{M_j}{M_i}\right)^{1/4}\right]^2 \tag{2.28}$$

The measured value of the viscosities of mixture using the equation is within the average deviation of 2%.

CHAPTER 3
METHODOLOGY & PROCEDURES

3.1 Methodology

In the modeling, the permeability of gas component is divided into 3 main mechanisms called Knudsen, viscous and surface effect. The summation of this effect results in the total permeability value.

3.1.1 Knudsen effect

a. Equation 2.1 is used to determine the permeability due to Knudsen effect. Knudsen effect is applicable only when the pore size is greater than the molecules size.
b. When the mean free path λ is small compared to the pore diameter d, molecule-molecule collision predominate and molecule-wall collision diminishes. Thus, according to equation 2.11, both Knudsen diffusivity and normal gas diffusivity are taken into account.
c. Molecular diffusivity is determined from equation 2.6 for binary mixture and 2.7 for multi component mixture. Generally, the molecular diffusivity can also be determined from equation 2.4 and 2.5. However, the parameters used (Lennard Jones constants and gas atomic volumes) are more complicated
d. Then, equation 2.10 is applied to calculate Knudsen diffusivity.

3.1.2 Viscous effect

a. Viscous permeability (equation 2.15) is strongly dependant of the respective gas viscosity.

b. Viscosity is for pure component is calculated using equation 2.16 and 2.17. Meanwhile viscosity of gas mixture is determined using equation 2.27 and 2.28.

3.1.3 Surface effect

a. ΔH_{ads} is the specific enthalpy difference of adsorption of gas species. In the absence of data, heat of adsorption can be estimated by Trouton's Rule of heat of vaporization (Equation 2.19 and 2.20).
b. Surface diffusivity and permeability are estimated using equation 2.18 and 2.21 respectively.
c. Another effect that should be considered is equilibrium loading factor, f which is represented by equation 2.22, 2.23 and 2.24. However, for this model the effect is neglected and the f value is assumed to be the inverse of membrane density.

3.1.4 Total permeability

a. The effect of Knudsen, viscous and surface are incorporated in the correlation for total permeability (Equation 2.25 and 2.26)
b. The permeability of pure component is determined by equation 2.25 and the permeability of gas mixture is determined by equation 2.26

3.2 Flow Diagram of Gas Permeability Algorithm

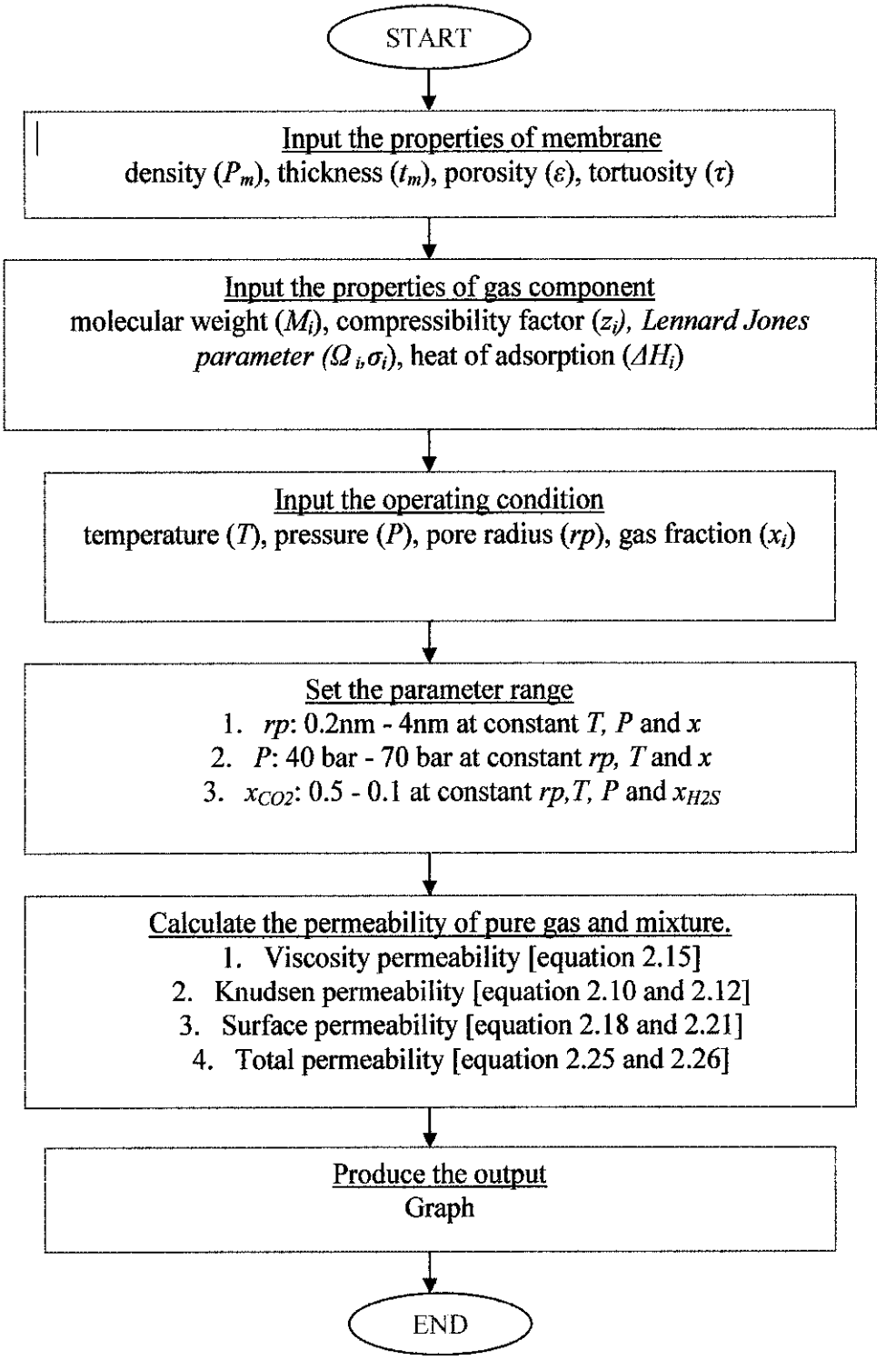

3.3 Model Development

3.3.1 Assumptions

- In order to derive a theoretical model for gas separation by membrane, the model is assumed to be in constant temperature (isothermal) and the pressure drop between the feed and permeate streams is neglected.

- Complete mixing of feed chamber and permeate chamber is assumed in the modeling of gas separation. In complete mixing model, the feed gas stream moves in plug flow parallel to the membrane surface whereas the permeate leaves the membrane in normal direction.

- Only physical type of adsorption is assumed to take place in the system. Thus, there is no chemical reaction occurs between the gas mixture. In some cases, the gas mixture tends to interact with one another. For example, interaction of water vapor always causes possible damage to the membrane.

- The system composes of rigid non-attracting spherical molecules with specific value of diameter and mass that moves freely.

- In the absence of equilibrium loading factor of gases on membrane surface, the factor is assumed to be the inverse of density.

3.3.2 Operating conditions

Lim Chin Han (2004) has conducted a study on binary mixture of carbon dioxide and methane using γ alumina membrane at T=363K and P=50bar. However at the respective condition, pure hydrogen sulfide does not exist as gases. Hence, simulation has been done using Hysys to determine the range of operating condition whereby all selected component co-exists in gas phases. Thus the range of condition that are feasible for this project are as follows:

Table 3.1 Operating conditions of modeling

Condition of feed	Effect	Pressure [bar]	Temperature [K]	Mol fraction	Pore radius [nm]
Pure	pore	50	363	1	0.1-4
	pressure	40-70	363	1	1
Binary • CO_2/CH_4 • H_2S/CH_4 • CO_2/H_2S	pore	50	363	0.3/0.7	0.1-4
	pressure	40-70	363	0.3/0.7	1
	concentration	50	363	0.1-0.9	
Tertiary • $CO_2/CH_4/H_2S$	pore	50	363	0.2/0.7/0.1	0.1-4
	pressure	40-70	363	0.2/0.7/0.1	1
	concentration	50	363	0.1-0.9	1

3.3.3 Data input

Fro the determination of gas component properties, the critical properties is necessary. the following table shows the critical properties of gases used in the modeling

Table 3.2 Critical value for selected compounds (Winnick, 1997)

Name	Formula	M.W	T_c, K	P_c, Bar	v_c, cc/mol	ω	z_c
Inorganic Compound							
Hydrogen sulfide	H_2S	34.04	373.2	89.4	98.6	0.081	0.184
Organic Compounds							
Methane	CH_4	16.043	190.6	46.0	99	0.007	0.288
Carbon dioxide	CO_2	44.01	304.1	73.8	93.9	0.225	0.274

3.34 Membrane selection

For this study, the same type of membrane as proposed by Lim Chin Han (2004) is used for the modeling which is the inorganic type of γ – alumina membrane is used for the modeling. This membrane is chosen because of its capability and suitability to separate carbon dioxide and hydrogen sulfide from natural gas.

Table 3.3: γ – alumina Membrane Properties (adapted from Lim Chin Han, 2004)

Membrane	Density, ρ_m (kg/m^3)	Thickness, t_m (μm)	Tortuosity, τ	Porosity, ε
γ - Alumina	3040	0.1	1.65	0.6

3.4 Tool Required: MATHCAD 12

MATHCAD 12 is an equation solving software that has a wide range of applicability to engineering problem. MATHCAD 12 is a logical choice when the requirements of the problem align with MATHCAD 12's strength, which included:

- Equations that are displayed in a highly readable form
- Ability to work with units and symbols
- An iterative solution capability and extensive function library
- Extensive ability to generate graph

Figure 3.1 shows the interface of MATHCAD as a compatible and user friendly mathematical software which can generate systematic result in tabulated form. There are also a lot of functions available in the tool box.

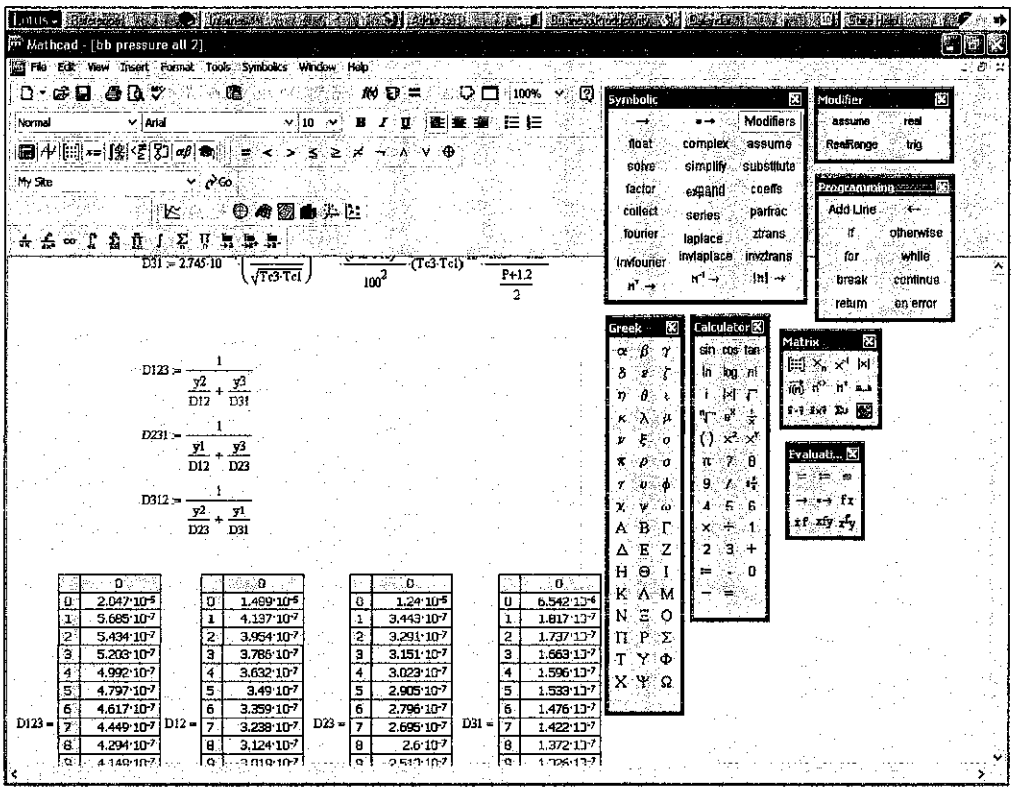

Figure 3.1: MATHCAD Interface

CHAPTER 4
RESULT AND DISCUSSION

4.1 Pure Component System

4.1.1 Effect of pore size

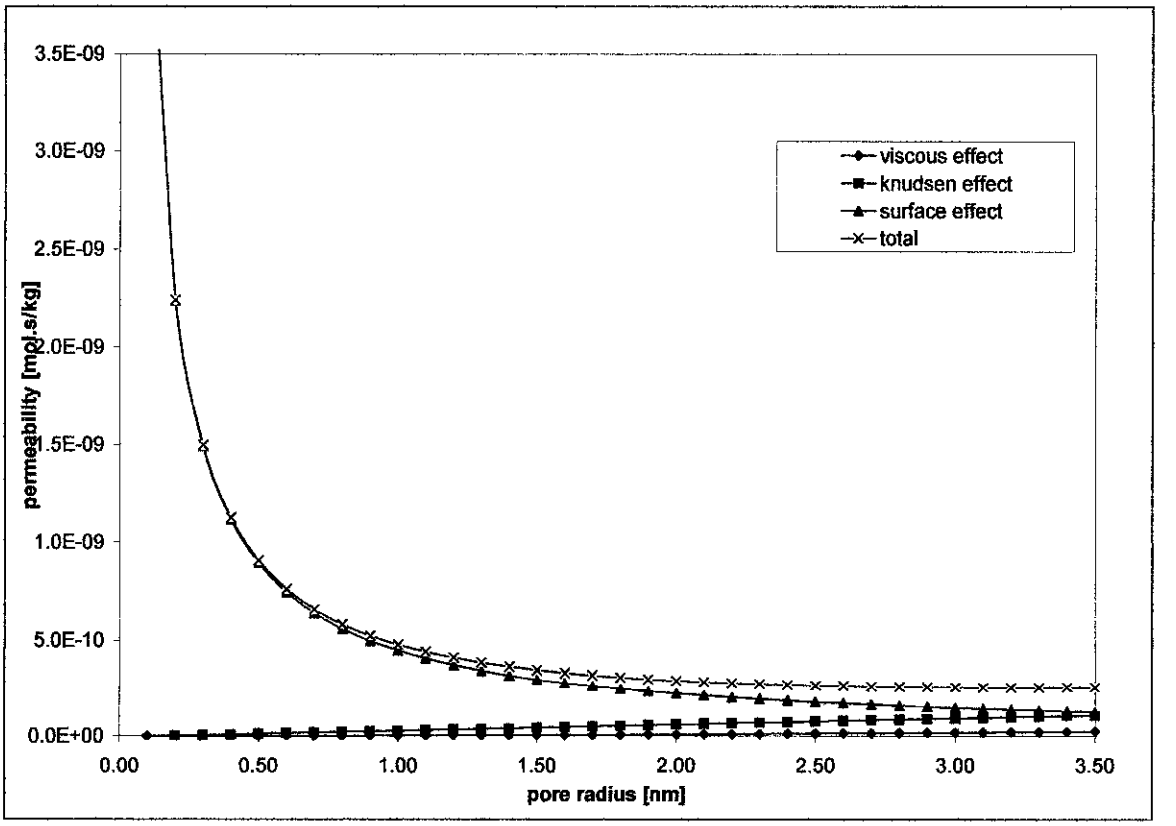

Figure 4.1: Permeability of pure carbon dioxide at P=60 bar and T=363K

There are three types of effects that contribute to the permeability of the gas components, namely Knudsen, viscous and surface effect. The most dominate type of effect for the separation is surface permeability and is shown in Figure 4.1. Surface adsorption is

noticeable in small diameter region. At this region, fast components which are carbon dioxide and hydrogen penetrate easily into the membrane and hinder the permeability of methane. Furthermore at low pore size, the collision between molecules is rarely occurred due to smaller pore size. The only driving force that causes the movement of gas molecules is the pressure gradient across the membrane. Basically, the adsorption of gas molecules into the surface is also dependent on the equilibrium loading factor, f and the density of membrane.

During the transportation of solute gas across membrane, the gas molecules accumulate and build up at the surface of the membrane. Concentration polarization occurs due to the pressure gradient. This results in higher convective transport of solute to the membrane. The concentration, *Cs* increases and gives larger back molecular diffusion of solute from membrane to bulk solution. Further increases in pressure drop increase the value of concentration, *Cs* to a limiting concentration.

The limit of the membrane to hold the molecules are called equilibrium loading factor. The factor can be approximated by using Henry Law to determine the solubility of gases or the uptake of gas species to the membrane and correlate it with the membrane capacity or density. However in the absence of this data for the respective membrane this factor is considered as 1 for all gases. The negligence of this factor causes the inaccuracy of data approximation since the each gas has different solubility on the membrane.

Knudsen diffusivity is effective when the pore diameter is higher than the gas molecule diameter. When the diameter of the pore increases, the gas tends to experience collision with the pore wall thus increasing the mean free path taken by the gas molecules. Generally, the Knudsen effect does not contribute much to the permeability rate because the mean free path taken by the molecules during collision is obviously longer than surface adsorption.

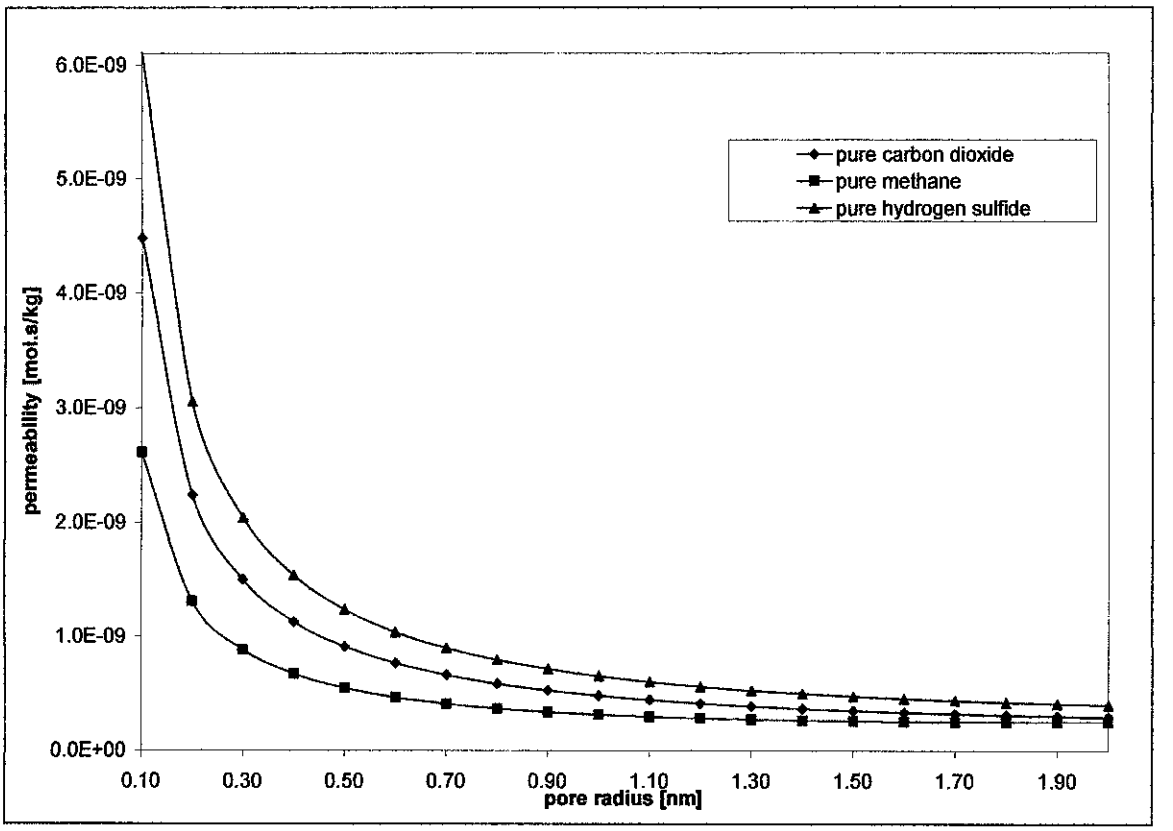

Figure 4.2: Permeability of pure component at P=60 bar and T=363K

Generally, the principle of membrane separation relies on the differences of the component permeation rates when they pass the membrane material. Due to the differences, the fast permeating species can be separated from slow permeating species. Based on the developed mathematical model, the permeation rate of each gas component can be estimated.

Based on the graph obtained (Figure 4.2), the permeability of hydrogen sulfide and carbon dioxide are proven faster than methane. This indicates that the separation at the respective condition is feasible. The most effective separation can be obtained at low pore radius. As the pore radius is increasing, the permeability of the component seems to be approaching each other. This phenomenon happens because as the pore size increases, more space is available for diffusion and the components tend to compete each other to pass through the membrane. Hence no selective permeability happens at large pore size.

Impurities in natural gas such as carbon dioxide and hydrogen sulfide should have distinctive permeability rates as compared to methane in order to achieve good separation. If the difference is so narrow, most of the methane will be lost in the permeate side. Basically, both carbon dioxide and hydrogen sulfide are classified as fast gas because they have smaller size as compared to methane. Due to the smaller size, the mobilization of gas molecules are more rapid, hence improve the separation.

Viscous effect is defined as the resistance of the gas molecules to flow. The effect is a function of inter molecules forces between molecules. In gases, momentum in transported by the molecules in free flight between molecules. Theoretically, the potential energy function of describing the interaction between spherical molecules state that when the distance of molecules is less than the molecules diameter, they will repel each other. Higher pore size also contributes to higher viscous effect besides Knudsen effect. This is because, as the pore size increases, the molecules have more space for collision with each other. Thus, the attraction and repulsion of molecules will become more significant.

4.1.2 Effect of pressure

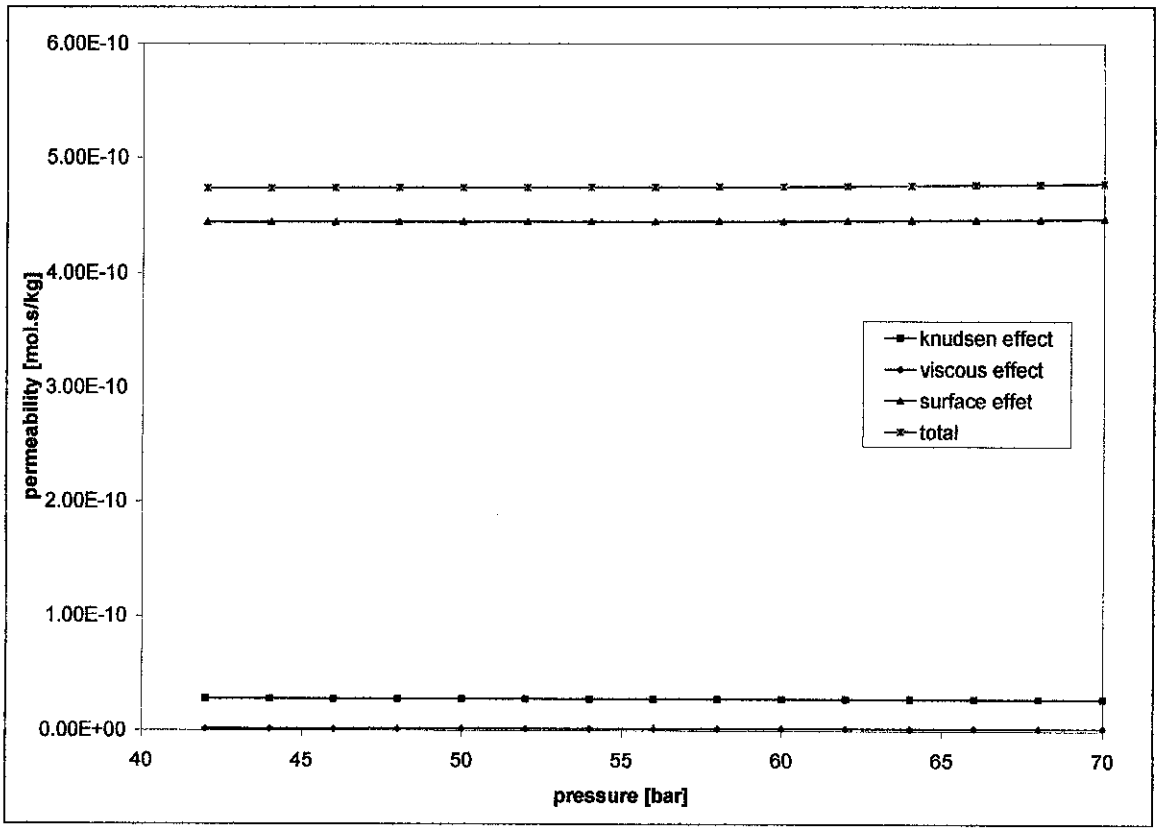

Figure 4.3: Permeability of pure carbon dioxide at T=363K and r_p=1nm

Generally at the selected pore size, surface effect predominates the permeability of gas component throughout the pressure gradient. Based on the permeability data of figure 4.3, Knudsen and viscous effect exert a little impact on the system.

The property that characterizes a fluid resistance to flow is called viscosity. The speed of flow through pores is inversely proportional to the viscosity. Theoretically, the viscosity of gases at low density increases with temperature roughly 0.6 to 1.0 power on the absolute temperature and is independent of pressure. Since the system is modeled at constant temperature, the viscosity of gas component remains constant as well. Therefore, from the graph, the permeability due to viscous effect remains constant.

The collision of molecules with the pore wall and the molecules is the implications of larger pore size as compared to molecules diameter. In a region of fixed pores, the mean free path taken of the molecules is constant. As a result permeability due to Knudsen effect lies horizontally along the plot.

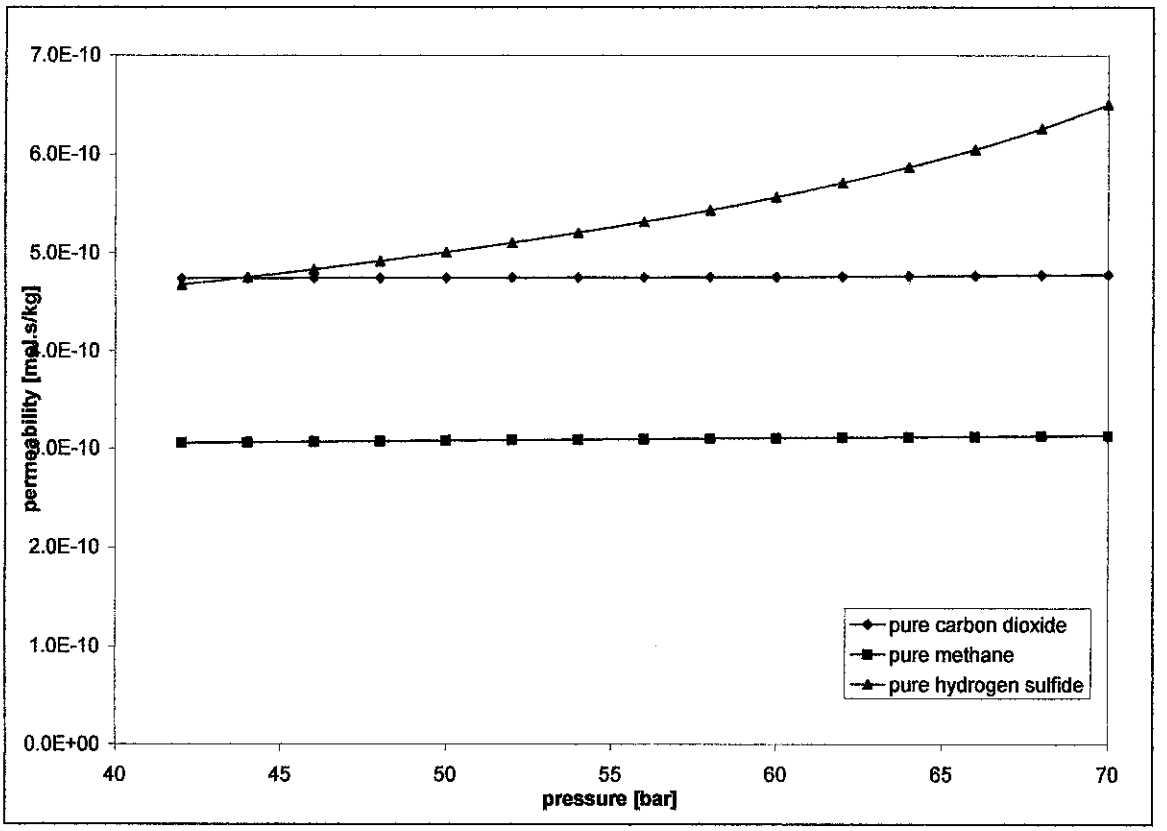

Figure 4.4: Permeability of pure components at T=363K and r_p=1nm

Generally, the permeability of hydrogen sulfide and carbon dioxide remains higher than methane with increasing pressure. In 1866, Graham formulated the solution diffusion process, where he postulated that the permeation process was independent of pressure. From figure 4.4, the pressure of both carbon dioxide and methane is visibly straight along the pressure difference. Since the permeability of both components is maintained constant throughout the increment of pressure, it is not economic to operate the system at high pressure.

However, a different trend line is observed from the hydrogen sulfide. Permeability of hydrogen sulfide is directly proportional to the pressure and is represented by slanting line. One of the possible reasons to cause this behavior is the value of hydrogen sulfide compressibility factor. Generally, at 363K, the compressibility factors of both carbon dioxide and methane are ranging from 0.9 to 0.99 when the pressure increases from 40 to 70 bar. But, the range of hydrogen sulfide compressibility factor is between 0. 8 and 0.5. Besides, at 363K hydrogen sulfide starts to condense when the pressure approaches 76 bar. Value of compressibility factor shows that hydrogen sulfide has a very significant deviation from ideal behavior particularly with the increment of pressure. Thus a wide range of compressibility factor causes the steepness in permeability slope.

4.2 Multi component system – Binary and Tertiary

4.2.1 Effect of pore size

In a binary mixture, the permeability of individual component is located in between the pure components permeability. In the case of CO_2/CH_4 mixture, the upper limit permeability is the permeability of pure carbon dioxide and the lower limit is the permeability of methane. While for the H_2S/CH_4 mixture, the permeability is restricted in between pure hydrogen sulfide and pure methane permeabilities.

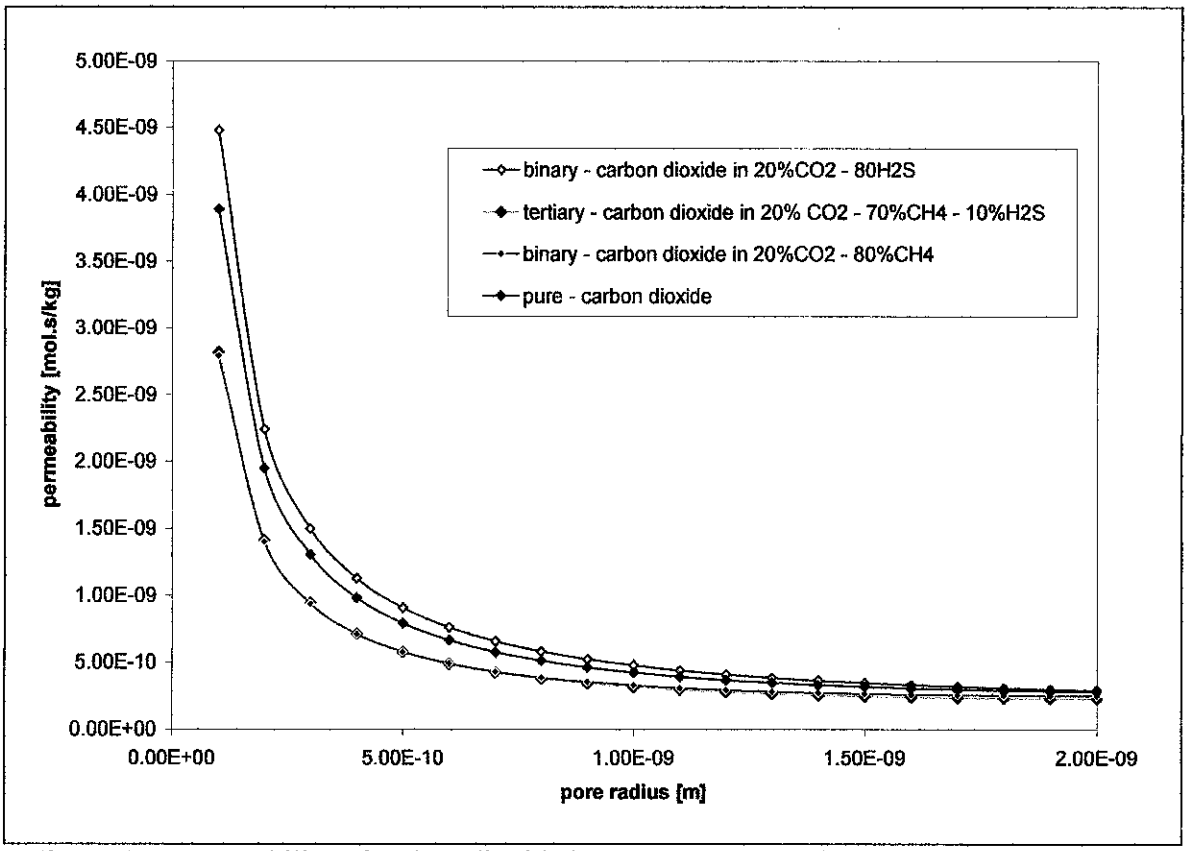

Figure 4.5: Permeability of carbon dioxide in pure component, binary and tertiary mixture at T=363K and P=60 bar

The permeability of carbon dioxide mixture is lower than the permeability of its pure component. From the figure, carbon dioxide has the lowest permeability in combination with methane. Since methane is classified as slow gas which has large molecule size, the

addition of methane reduced the mobility of carbon dioxide. Methane molecules tend to hinder the movement of carbon dioxide. Carbon dioxide is observed to have higher permeability rate when it mixes with hydrogen sulfide. Generally, hydrogen sulfide which has greater permeability that carbon dioxide enhances the permeability of carbon dioxide. For tertiary mixture of 30%CO_2-60%CH_4-10%H_2S, the permeability is found higher than binary mixture of 30%CO_2-70%CH_4 due to the addition of hydrogen sulfide.

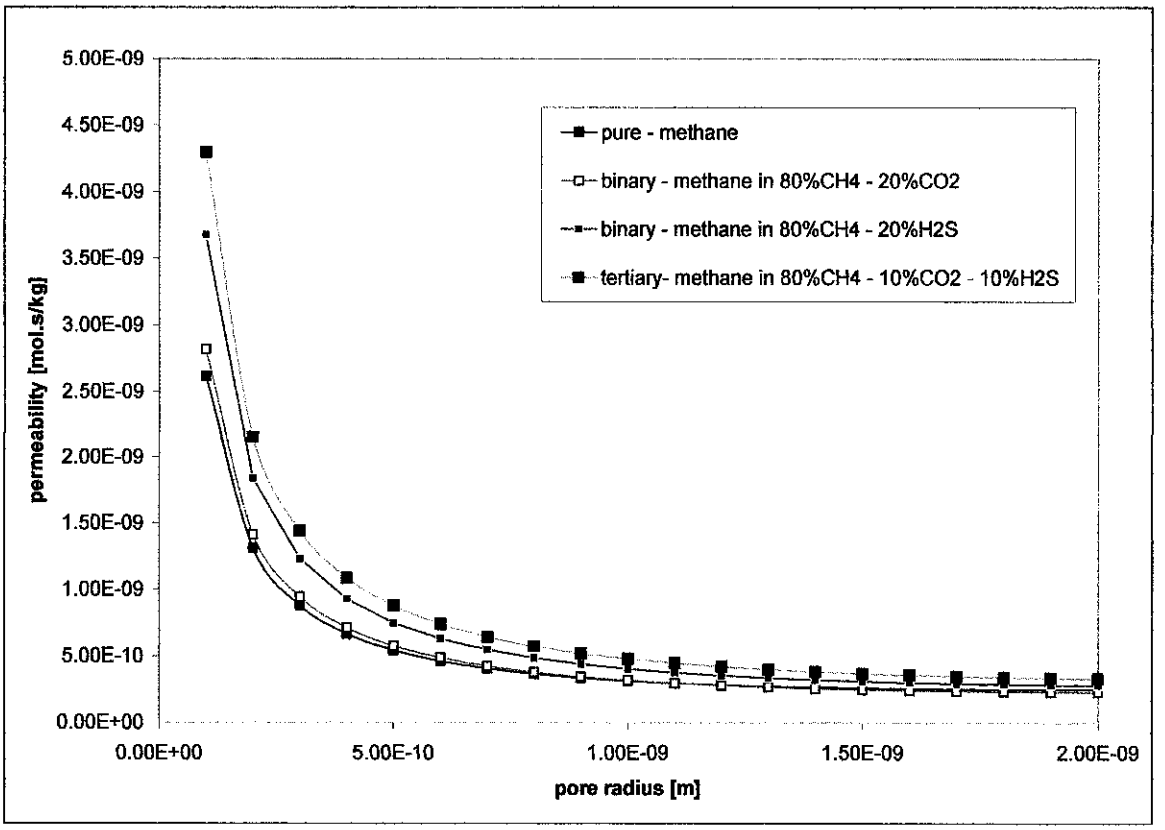

Figure 4.6: Permeability of methane in pure component, binary and tertiary mixture at T=363K and P=60 bar

Figure 4.6 indicates that as the permeability of methane is dependent on the concentration of carbon dioxide and hydrogen sulfide that exists in the system. The increment of carbon dioxide and hydrogen sulfide in methane increase the permeability rate of methane. These impurities help to speed up the slow movement of methane thus increasing its permeability across the membrane. On the other hand, the permeabilities of both impurities decrease with the increment of methane in the binary mixture.

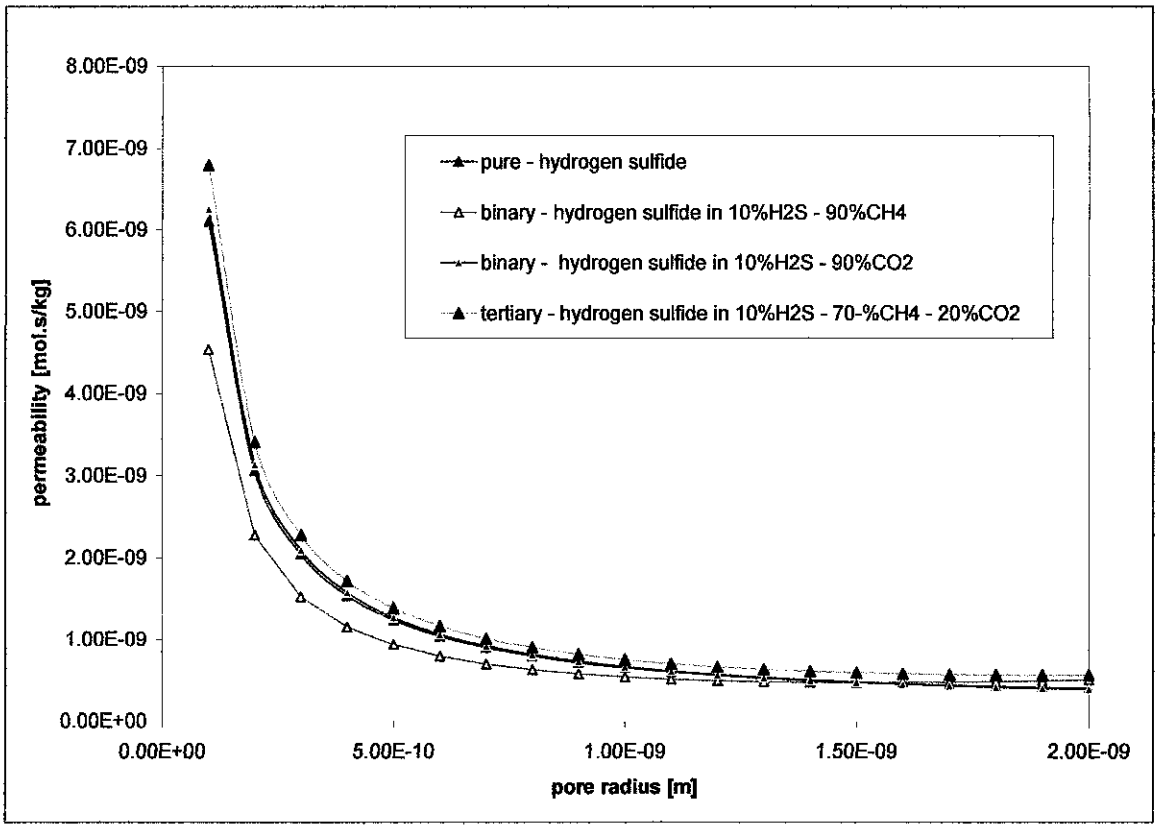

Figure 4.7: Permeability of hydrogen sulfide in pure component, binary and tertiary mixture at T=363K and P=60 bar

Figure 4.7 indicates that the permeability of H_2S/CH_4 mixture is very slow as compared to other combination. As explained before, the existence of methane hinders and delays the permeability rate of hydrogen sulfide.

However, a unique behavior is modeled from the combination of H_2S/CO_2 mixture. Based on the model, the permeability of hydrogen sulfide is found higher than its pure component permeability rate. Since both gases are classified as slow gas with high solubility, hydrogen sulfide can easily diffuse in carbon dioxide. The quick movement of these slow gases is expected to increase to permeability of hydrogen sulfide.

4.2.2 Effect of pressure

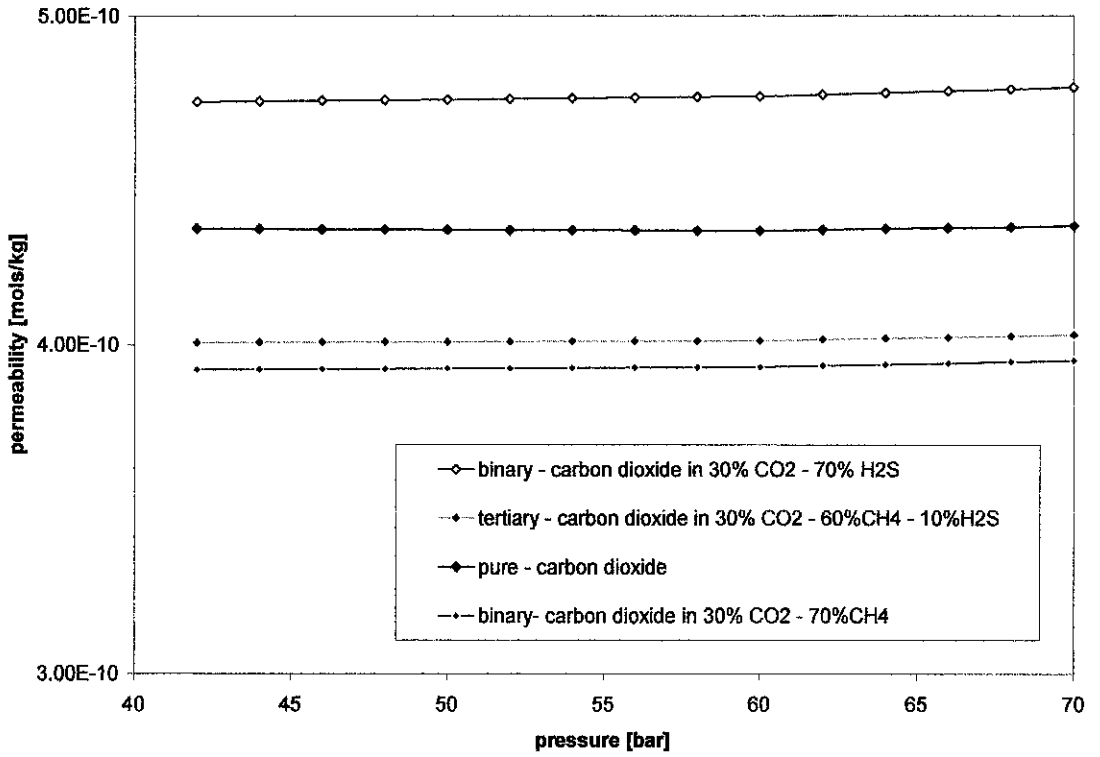

Figure 4.8: Permeability of carbon dioxide against pressure for pure component, binary and tertiary mixture at T=363K and r_p=1nm

Figure 4.8 represents the comparison of pure component with binary and tertiary mixture permeability at various combinations.

Permeability of carbon dioxide in CO_2/CH_4 is lower, relative to pure component. The permeability of this combination is restricted by the pure carbon dioxide permeability as the upper limit and methane permeability as the lower limit. Thus the permeability of carbon dioxide in binary mixture is estimated to be lower than the pure component.

In CO_2/H_2S mixture, the permeability of carbon dioxide is higher that pure component. Molecular diffusion can be defined as the transfer or movement of individual molecules through a fluid by means of random individual movement of molecules. Theoretically, the diffusion of molecules is driven by the concentration gradient in a stationary bulk fluid. In this case, carbon dioxide which has lower percentage is predicted to diffuse into the bulk hydrogen sulfide, thus affecting the diffusivity value of the system. Basically, the diffusivity of molecules is inversely proportional to pressure. Since both gases are classified in fast category, the permeability rate is so much higher as compared to other combination. For tertiary mixture, carbon dioxide permeability is higher than binary CO_2/CH_4 mixture due to the addition of hydrogen sulfide.

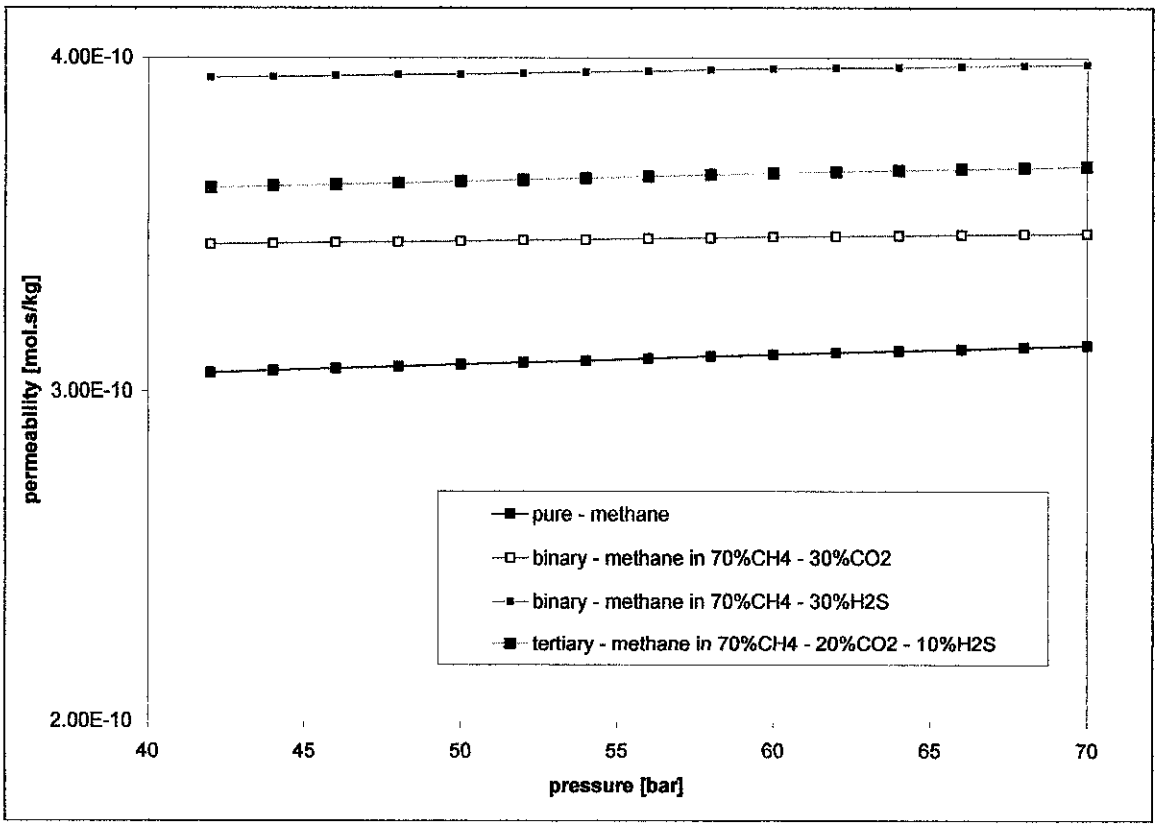

Figure 4.9: Permeability of methane against pressure for pure component, binary and tertiary mixture at T=363K and r_p=1nm

Permeability of methane is very slow in pure condition. The permeability increases with the addition of impurities such as carbon dioxide and hydrogen sulfide. Permeability methane in tertiary mixture is estimated to be in between binary CH_4/CO_2 and $CH_4/H2_S$. Permeability of methane in multi component mixture is higher than its pure component. However, contrary effect is observed in carbon dioxide and hydrogen sulfide permeability.

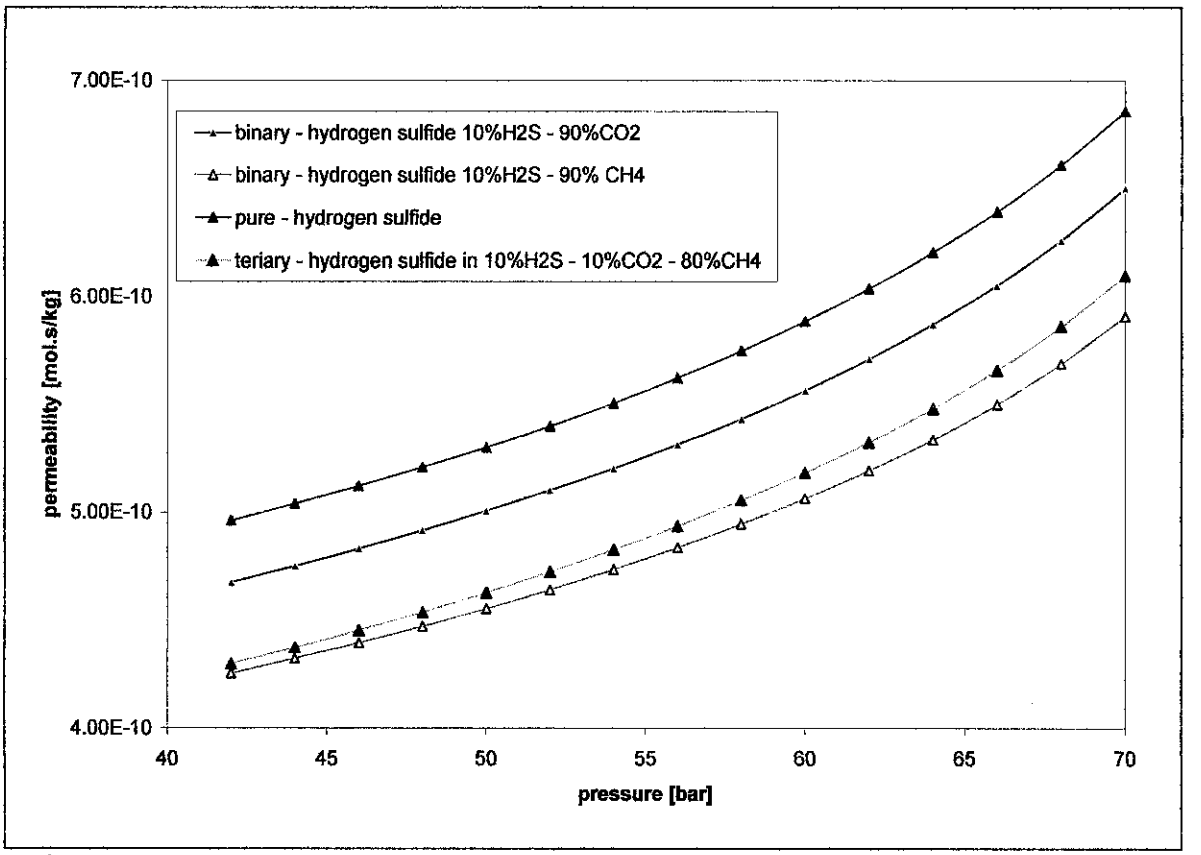

Figure 4.10: Permeability of hydrogen sulfide against pressure for pure component, binary and tertiary mixture at T=363K and r_p=1nm

Figure 4.10 shows that permeability hydrogen sulfide in combination of methane mixture is slower than its pure component for both binary and tertiary. However, the permeability of hydrogen sulfide is found higher with the combination of carbon dioxide. Permeability of hydrogen sulfide across membrane is dependent n pressure. When more pressure is exerted on the system, more hydrogen sulfide is forced to penetrate into the membrane, but the permeability of methane and carbon dioxide remains constant. Hence, for a binary mixture of hydrogen sulfide and methane, separation should be done at high operating pressure.

However, further increment of pressure approaching dew point will cause condensation of hydrogen sulfide. If liquid is present in the gas separating process, a liquid film can increase the membrane resistance markedly. Liquid can also damage the membrane by chemical action or by swelling or softening. Therefore it is important to the study the allowable range of pressure at isothermal condition to prevent condensation of gas.

4.2.3 Effect of Concentration

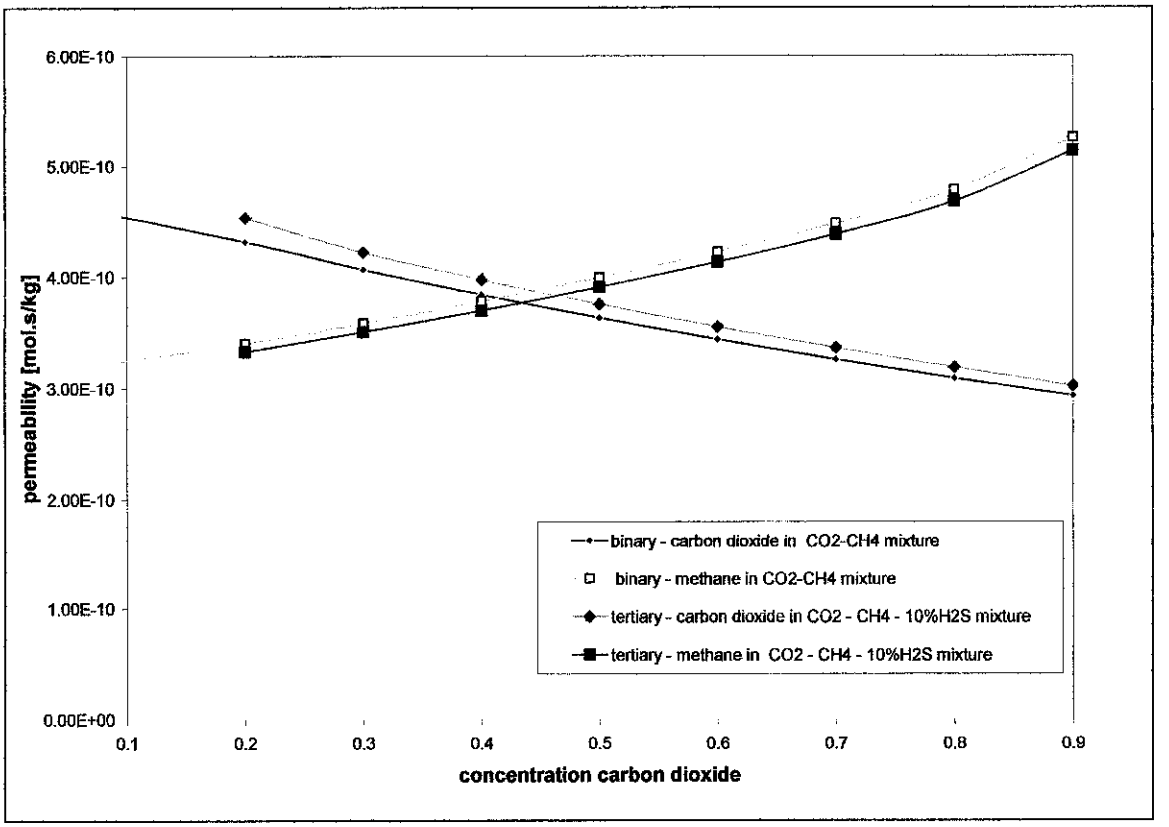

Figure 4.11: Permeability of carbon dioxide and methane at T=363K, P=60bar and r_p=1nm

Figure 4.11 shows the concentration profile of binary and tertiary component. Carbon dioxide can be removed easily at low carbon dioxide concentration due to the selectivity of the carbon dioxide permeability. Within that particular operating conditions and assumptions, the separation is possible at lower concentration of carbon dioxide and

hydrogen sulfide. If the concentration of carbon dioxide is found higher than 0.4, the separation process will be difficult because the permeability of carbon dioxide is drastically reduced as its concentration increases.

Therefore, in order to achieve good separation, impurities composition should be lower.

4.3 Selectivity at various pore size and various pressure

4.3.1 Pore size

For this model, the selectivity is determined for the most dominant component which are carbon dioxide and methane. in this case, hydrogen sulfide is assumed to have equal or greater permeability than carbon dioxide, thus having higher selectivity. As the consequence, it is expected to permeate faster.

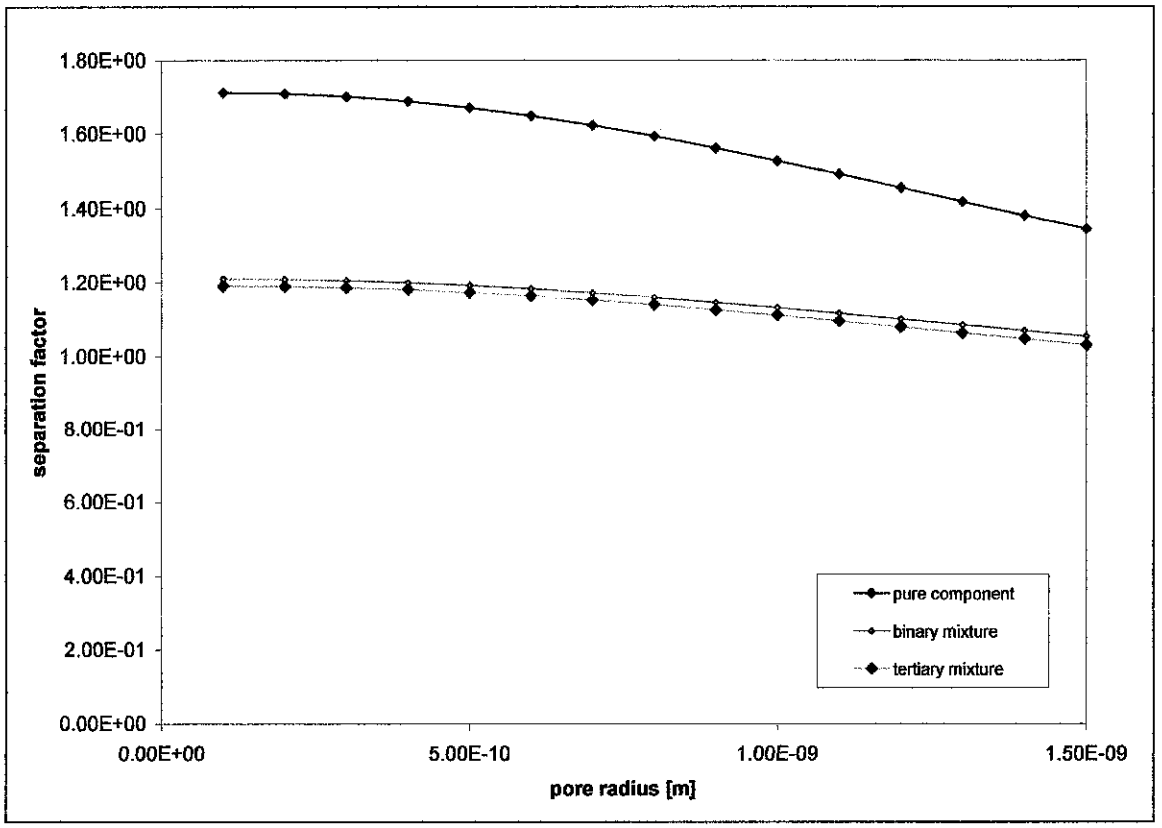

Figure 4.12: Selectivity of carbon dioxide / methane at T=363K, P=60bar

In order to obtain a good separation, the selectivity of impurities over natural gas should be reasonably higher since the principle of membrane separation is the difference of two permeability rate. Though, one limitation of this model is the negligence of equilibrium

loading factor or also known as solute solubility into the adsorbent. The constraint is due to the non-extended study of equilibrium loading factor for that particular membrane.

Based on the Henry's Law constant which is used to approximate the solubility of the gas components in water, the solubility of methane differs from the solubility of carbon dioxide and hydrogen sulfide by magnitude of 24 and 74 respectively. Basically, the equilibrium loading factor is an important for accurate modeling of real behavior. However, this study focused on construction of the simplest model for early prediction of gas separation. This model actually provides the minimum permeability values posses by the system by predicting the range of suitable operating condition and trend line of individual gas component.

4.3.2 Pressure

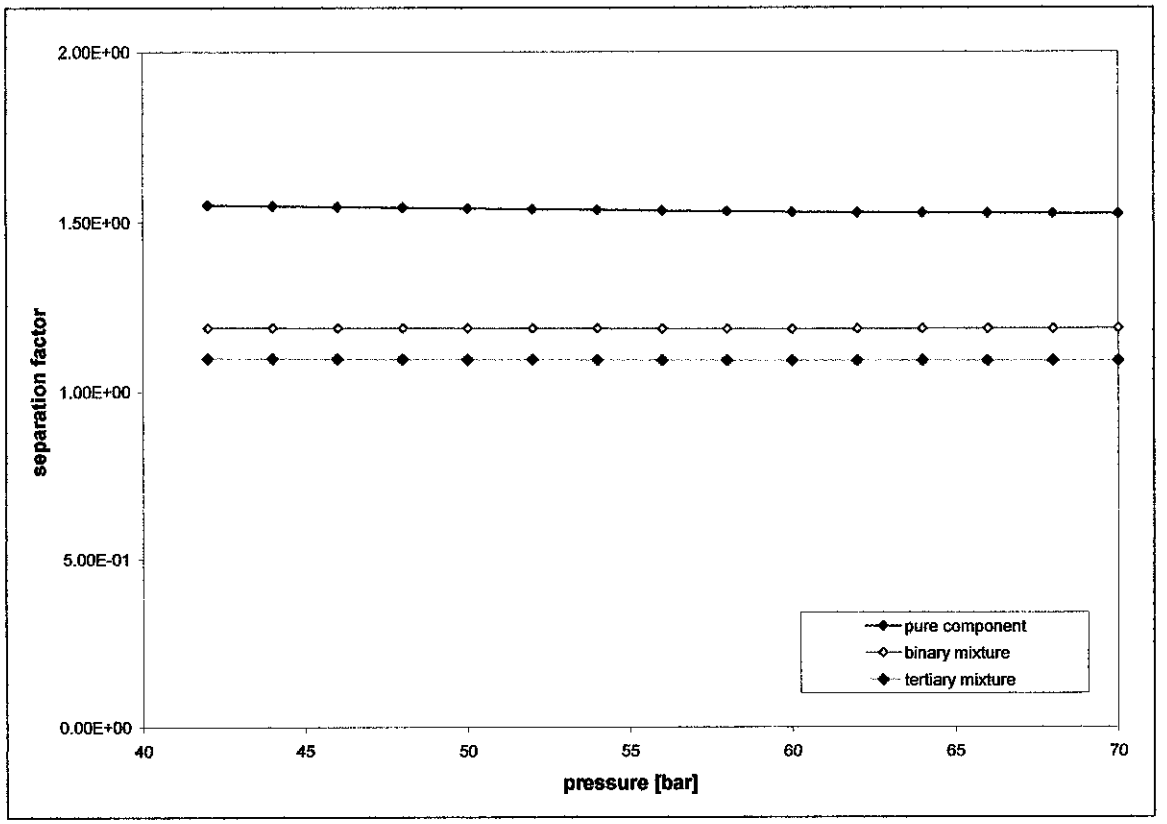

Figure 4.13: Selectivity of carbon dioxide / methane at T=363K, P=60bar

Overall, the separation factor of carbon dioxide / methane decreases as the system deviates from the pure component. The existence of fast gas impurities tends to increase the permeability of methane but lower the selectivity. It means that, there will be some amount of impurities permeate into the retentate side and some amount of methane loss in the permeate side.

According to the early prediction of the separation system behavior, the most suitable operating pressure for carbon dioxide – methane – hydrogen sulfide is 40 bar. Through out the modeling, the temperature is maintained at 363 K in order ensures that all components co-exist as gases since hydrogen sulfide easily liquefy. From figure 4.12 the most optimum selectivity of obtained at low pore size. Hence the smaller pore size is preferable to achieve good separation

CHAPTER 5
CONCLUSION

1. Permeability of hydrogen sulfide is the highest followed by carbon dioxide and methane respectively. The permeability of binary mixture of CO_2/CH_4, H_2S/CH_4 and CO_2/H_2S depends on combination of gases in the mixture. Basically the permeability of faster gas will decrease with the addition of slow gas. On the contrary, the permeability of slow gas is predicted to be improved due to the combination with fast gas. The same trend is observed for the permeability gas in tertiary mixture. The model also shows that permeability of hydrogen sulphide increases as the pressure increased. However, the permeability of carbon dioxide and methane is independent of pressure.

2. The most effective separation can be obtained at low pore radius The permeability of hydrogen sulfide and carbon dioxide are faster than methane.. As the pore radius is increasing, the permeability of the component tends to approach each other and thus causes a tighter gap between permeability rates. There are three types of effects that contribute to the permeability of the gas components, namely Knudsen, viscous and surface effect. The most dominate type of effect observed from the modeling is surface permeability

3. The permeability of hydrogen sulfide and carbon dioxide are faster than methane with increasing pressure. Permeability of carbon dioxide and methane is maintained constant throughout the increment of pressure. However, the permeability of hydrogen sulfide is increases proportional to the pressure. Steepness of hydrogen sulfide permeability happens due to the wide variation of compressibility factor as a result of deviation from ideal gas.

4. Increment of methane impurities in the mixture will reduce the permeability rate of carbon dioxide. On the other hand, the permeability of methane increases with the addition of carbon dioxide. Since methane is classified as slow gas which has large molecule size, the addition of methane reduced the mobility of carbon dioxide and vice versa. Existence of a small amount of hydrogen sulfide into the system increases the mobility of carbon dioxide and methane because of the fast nature of hydrogen sulfide.

5. Within the selected operating conditions and assumptions, the concentration by which separation can occur for binary and tertiary system (carbon dioxide – methane and carbon dioxide- methane –hydrogen sulfide) is 40% mol carbon dioxide. If the mol fraction of carbon dioxide is found higher than 0.4, the separation process will be impossible because the permeability of carbon dioxide is drastically reduced as its concentration increases.

6. The most optimum selectivity of carbon dioxide / methane is obtained at low pore size. While the most suitable operating pressure for carbon dioxide – methane – hydrogen sulfide separation is 40 bar. Through out the modeling, the temperature is maintained at 363 K in order ensures that all components co-exist as gases since hydrogen sulfide easily liquefy.

CHAPTER 6
RECOMMENDATION

1. For this study, the equilibrium loading factor is not taken into account due to the absence of literature data. Solute loading on the adsorbent which is expressed in mass, mol or volume per unit mass can be predicted by experiment or by application of Freundlich and Langmuir Isotherm. Thus it is necessary to obtain experimental data equilibrium data for a particular solute or solvent. A plot of solute loading versus concentration or partial pressure called adsorption isotherm is necessary to determine the amount of solute adsorbed from a given gas components. When the amount adsorbed is assumed to be low, the isotherms are almost linear and can be estimated using Henry's Law. Generally, this model is only suitable for early prediction of gas separation due to the negligence of equilibrium loading factor.. Based on the Henry's Law constant which is used to approximate the solubility of the gas components in water, the solubility of methane differs from the solubility of carbon dioxide and hydrogen sulfide by magnitude of 24 and 74 respectively. Thus, the consideration on equilibrium factor will increase the selectivity of component.

2. Monolayer membrane is the simplest structure of membrane technology. In order to eliminate the drawback in monolayer membrane, multilayer membrane is produced. It consists of a thin selective layer made of one polymer mounted on an asymmetric membrane, which is composed of another polymer. This composite structure allows the optimization of required separation for the selective layer. Therefore, it is recommended to study the comparison between monolayer and multilayer membrane in natural gas separation.

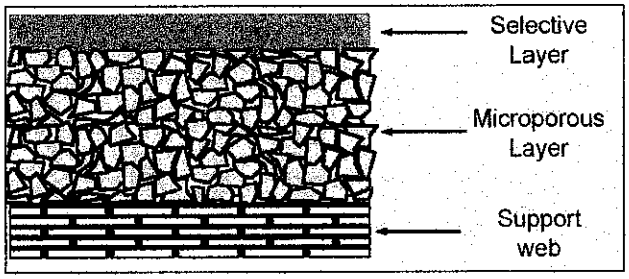

Figure 6.1: Example of monolayer membrane

3. Multistage operation is very common applied in the industry. In high carbon dioxide removal applications, a significant amount of hydrocarbons that permeate through membrane and are lost. Hence, multistage systems are implemented to recover a portion of these hydrocarbons. The portion of first-stage permeate that is lost is usually taken to be recycled at low pressure and is repressurized before combining with the feed gas. Thus, it is very significant to study the characteristic of multistage separation that is widely used in industry.

4. Currently the modeling is done up tot tertiary components system. In order to get better overview of the separation, it is advisable to model a real composition of untreated natural gas. The study of multi component system with consideration to the real industrial problem is more practical to gain the better understanding regarding this field.

REFERENCES

1. Hilmi Mukhtar, Lim Chin Han (2004). Permeability Studies of Carbon Dioxide and Methane Across y-alumina Membrane. Proceedings of the 18th Symposium of Malaysian Chemical Engineers, 2, 101-107

2. P. J. H. Carnell and G. Towler (1997). Ultra-Purification of Natural Gas and NGLs Using a Novel Low Energy Process for the Removal of CO_2 and H_2S. Proceedings ASCOPE 97 Conference.

3. Jose Mugge, Hans Bosch, Tom Reith (2003). Measuring and Modeling of Gas Adsorption Kinetics in Single Porous Particles. Chemical Engineering Science, 56, 5351-5360

4. Richard W. Baker (2001). Future Direction of Membrane Gas Separation Technology. Industrial & Engineering Chemical Research, 41, 1393-1411

5. David T. Coker, Rajeev Prabhakar, Benny D. Freeman (2003). Tool for Teaching Gas Separation Using Polymers. Chemical Engineering Education Volume 37, 1, 60

6. Chien-Chieh Hu, Chin-Shun Chang, Ruoh-Chyu Ruaan, Juin-Yih Lai (2003). Effect of free volume and sorption on membrane gas transport, Retrieved March 15, 2005, from the World Wide Web: http://www.sciencedirect.com

7. Subrata Roy , Sarah M. Cooper , M. Meyyappan , Brett A. Cruden (2005). Single component gas transport through 10 nm pores; Experimental data and hydrodynamic prediction, Journal of Membrane Science. Retrieved March 15, 2005, from the World Wide Web: http://www.sciencedirect.com

8. Shiguang Li, Guerro Alvarado, Richard D. Noble, John L. Falconer (2005). Effect of impurities on CO2/CH4 separation through SAPO-34 Membrane; Journal of

Membrane Science. Retrieved March 15, 2005, from the World Wide Web: http://www.sciencedirect.com

9. Lars Kucka, Ivo Muller, Eugeny Y., Kenig Andrzey Gorak (2003). On the Modeling and Simulation of Sour Gas Absorption by Aqueous Amine Solution. Chemical Engineering Science, 58, 3571-3578

10. T. L. Chan and S. Miskon (2004). A Review of Technology Challenge in Liquefied Natural Gas Processes. Proceedings of the 18th Symposium of Malaysian Chemical Engineers, 2, 89-93

11. T. L. Ng, M.S.Shaharun, P.N.F Megat Khamaruddin, F.K.Chong, N.Y.Yuhana. N. Mohd Yunus, V.R.Radhakrishnan (2004). Zero CO_2 Emissions in Natural Gas Processing. Proceedings of the 18th Symposium of Malaysian Chemical Engineers, 2, 81-88

12. A.S Azmi, Putri N. Faizura. Ng. T. L., V. R. Radhakrishnan (2004). Carbon Dioxide Absorption in Cocurrent Contactors – Review of Current Status and Research Opportunities. Proceedings of the 18th Symposium of Malaysian Chemical Engineers, 2, 108-114

13. David Dortmundt, Kishore Doshi (1999). Recent Developments in CO_2 Removal Membrane Technology, UOP LLC.

14. Sami Matar and Lewis F. Hatch (2001). Chemistry of Petrochemical Process, Second Edition, Chapter 1, 1-26

15. J. D. Seader, Earnest J. Henley (1998). Separation Process Principle, United States, John Wiley and Sons Inc

16. Christie John Geankoplis (2003). Transport Process and Separation Process Principle, fourth Edition, Prentice Hall.

17. Norman J. Hyne (2001). Petroleum Geology, Exploration, Drilling and Production, Second Edition, PennWell Corporation.

18. K. Li, Jianfeng Kong, Xiaoyao Tan (2000). Design of Hollow Fibre Membrane Modules for Soluble Gas Removal. Chemical Engineering Science, 55, 5579-5588

19. Richard W. Baker, A. R. Da Costa, D. E. Gottsclich, M. L. Jacobs, K. A. Lokhandwala, A. P. Mairal, I. Pinnau, J. G. Wijmans (2003). Membrane for Hydrocarbon Recovery in Petrochemical, Refinery and Natural Gas Processing Application. Membrane Technology Research Inc. Retrieved Feb 12, 2005, from the World Wide Web: http://www.mtrinc.com/

20. BP Statistical Review of World Energy (2004, June). Retrieved Feb 12, 2005, from the World Wide Web: http://www.bp.com/worldenergy/

21. Nun Zuraini Zailani (2003), Separation of Hydrogen Sulfide from Methane by using Membrane Technology. University Teknologi Petronas.

APPENDICES

APPENDIX 1

Gantt Chart

Activities	Week													
	1	2	3	4	5	6	7	8	9	10	11	12	13	14
Topic Proposal & Finalization														
Preliminary Research & Literature Review														
Submission of Preliminary Report														
Modeling Work & Continuation of Literature Review														
Submission of Progress Report														
Continuation of Modeling Work														
Submission of Dissertation Final Draft														
Oral Presentation														
Submission of Project Dissertation														

APPENDIX 2

Compressibility Data
(adapted from Perry's Chemical Engineering Handbook)

Compressibility Factor			
P	methane	carbon dioxide	hydrogen sulfide
40	0.9662	0.9938	0.7946
42	0.9648	0.9936	0.7826
44	0.9634	0.9933	0.7703
46	0.9619	0.9931	0.7577
48	0.9605	0.9928	0.7448
50	0.9591	0.9926	0.7315
52	0.9577	0.9924	0.7179
54	0.9563	0.9921	0.7038
56	0.9548	0.9919	0.6892
58	0.9534	0.9916	0.6741
60	0.9520	0.9914	0.6584
62	0.9508	0.9904	0.6419
64	0.9496	0.9894	0.6246
66	0.9484	0.9884	0.6062
68	0.9472	0.9874	0.5864
70	0.9461	0.9864	0.5649
72	0.9449	0.9854	0.5411
74	0.9437	0.9844	0.5136
76	0.9425	0.9834	
78	0.9413	0.9824	
80	0.9401	0.9814	

APPENDIX 3

Viscosity data for pure hydrogen sulfide simulated by HYSYS

Temperature	Viscosity ($N.s/m^2$) at Various Pressure(bar)											
°C	40	45	50	55	60	70	75	80	85	90	65	100
30												
40												
50	2.1088E-04											
60	1.5010E-05	1.9747E-04	1.9820E-04									
70	1.5298E-05	1.5645E-05	1.6078E-05	1.8453E-04	1.8552E-04							
80	1.5607E-05	1.5912E-05	1.6272E-05	1.6715E-05	1.7293E-05	1.7220E-04	1.7350E-04					
90	1.5930E-05	1.6204E-05	1.6519E-05	1.6887E-05	1.7331E-05	1.8647E-05	1.9864E-05	1.5410E-04	1.5674E-04			
100	1.6263E-05	1.6514E-05	1.6796E-05	1.7116E-05	1.7487E-05	1.8458E-05	1.9136E-05	2.0069E-05	2.1641E-05	1.2073E-04	1.3338E-04	1.3892E-04
110	1.6604E-05	1.6836E-05	1.7093E-05	1.7380E-05	1.7703E-05	1.8498E-05	1.9002E-05	1.9614E-05	2.0385E-05	2.1443E-05	2.3030E-05	2.5799E-05
120	1.6951E-05	1.7168E-05	1.7405E-05	1.7666E-05	1.7955E-05	1.8640E-05	1.9052E-05	1.9527E-05	2.0083E-05	2.0747E-05	2.1568E-05	2.2647E-05

gas liquid

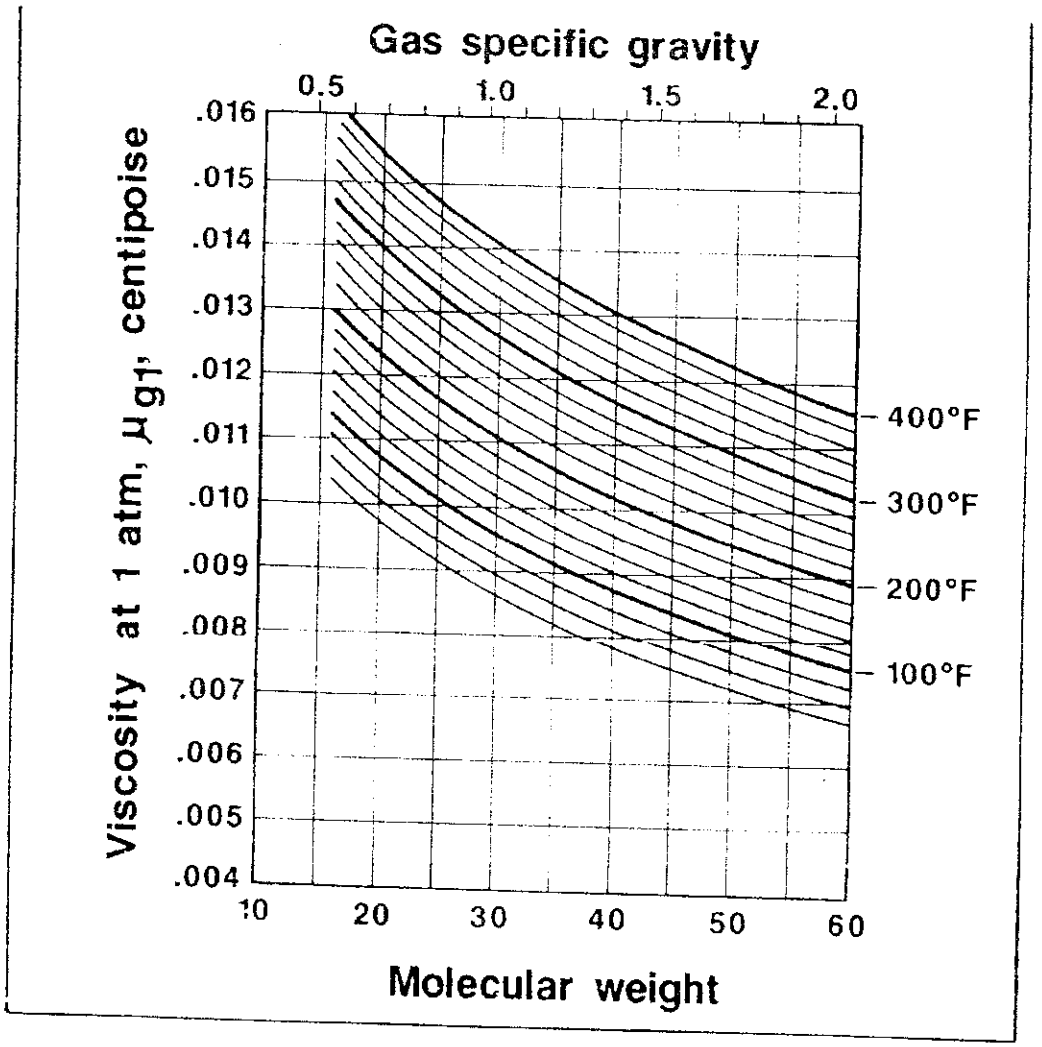

Fig. 6–8. Viscosities of natural gases at atmospheric pressure. (Adapted from Carr et al., *Trans.*, AIME, *201*, 997.)

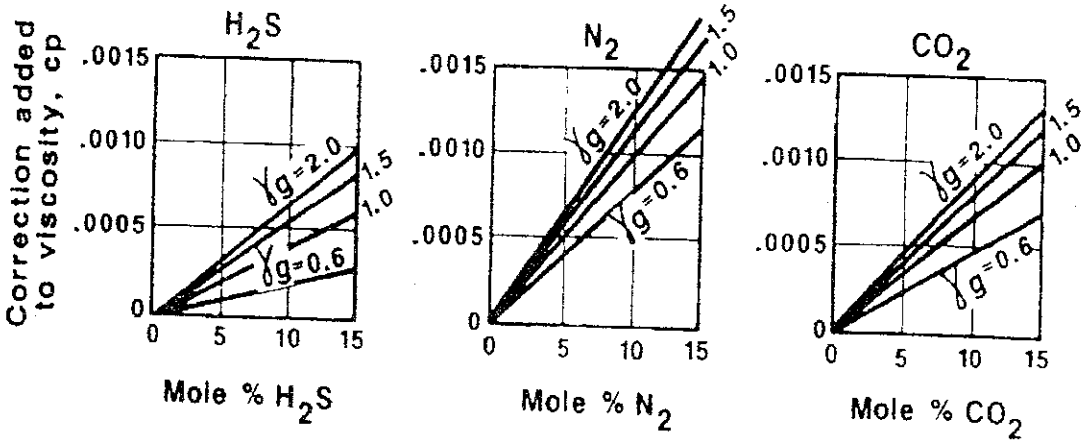

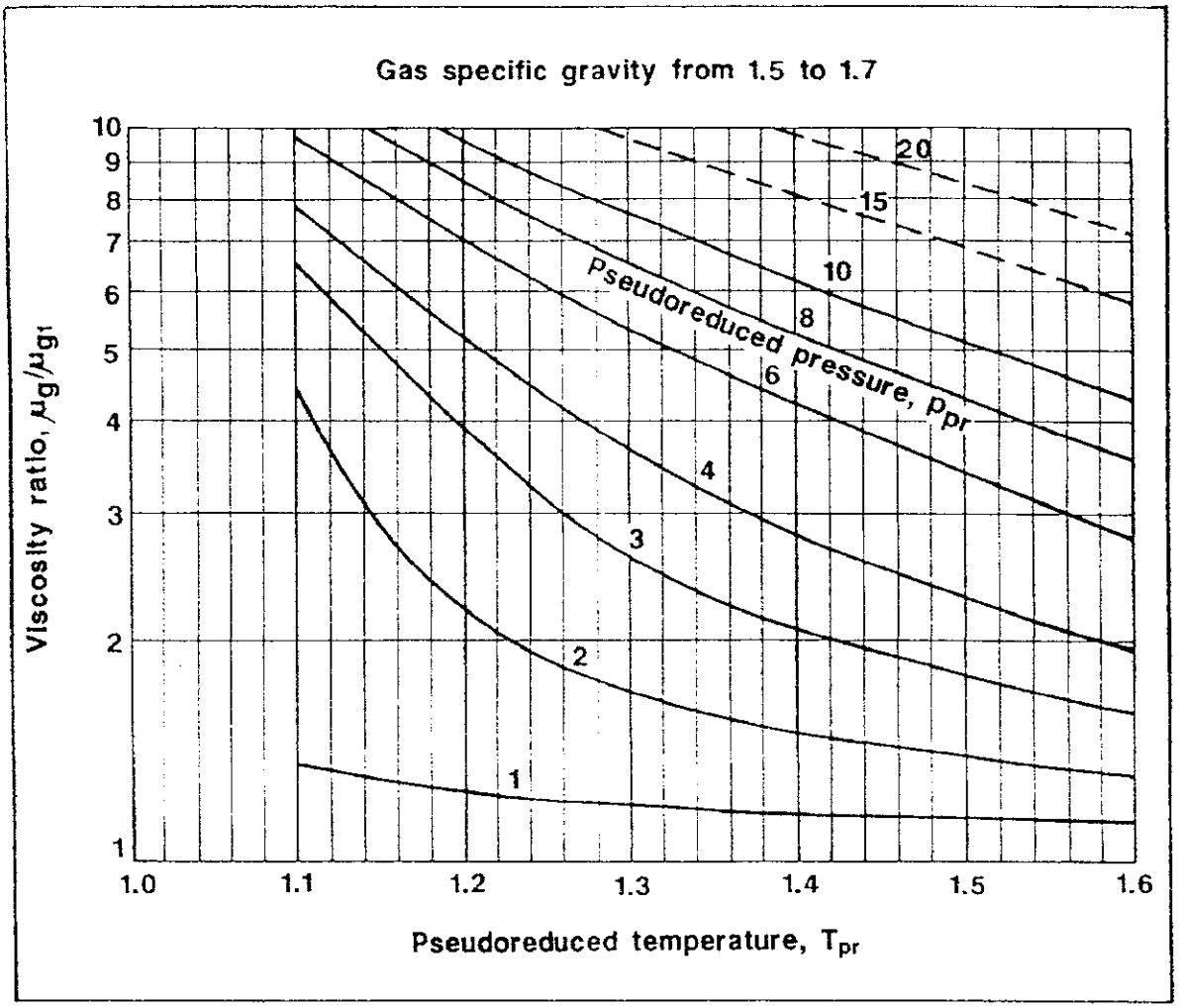

Fig. 6–12. Viscosity ratios for natural gases with specific gravities from 1.5 to 1.7.

APPENDIX 4

Substance	Molecular Weight M	Lennard-Jones parameters σ (Å)	ε/κ (K)	Ref.	Critical properties[g,h] T_c (K)	p_c (atm)	$\tilde{V}_c$ (cm³/g-mole)	μ_c (g/cm · s × 10^6)	k_c (cal/cm · s · K × 10^6)
Light elements:									
H_2	2.016	2.915	38.0	*a*	33.3	12.80	65.0	34.7	—
He	4.003	2.576	10.2	*a*	5.26	2.26	57.8	25.4	—
Noble gases:									
Ne	20.180	2.789	35.7	*a*	44.5	26.9	41.7	156.	79.2
Ar	39.948	3.432	122.4	*b*	150.7	48.0	75.2	264.	71.0
Kr	83.80	3.675	170.0	*b*	209.4	54.3	92.2	396.	49.4
Xe	131.29	4.009	234.7	*b*	289.8	58.0	118.8	490.	40.2
Simple polyatomic gases:									
Air	28.964[i]	3.617	97.0	*a*	132.4[i]	37.0[i]	86.7[i]	193.	90.8
N_2	28.013	3.667	99.8	*b*	126.2	33.5	90.1	180.	86.8
O_2	31.999	3.433	113.	*a*	154.4	49.7	74.4	250.	105.3
CO	28.010	3.590	110.	*a*	132.9	34.5	93.1	190.	86.5
CO_2	44.010	3.996	190.	*a*	304.2	72.8	94.1	343.	122.
NO	30.006	3.470	119.	*a*	180.	64.	57.	258.	118.2
N_2O	44.012	3.879	220.	*a*	309.7	71.7	96.3	332.	131.
SO_2	64.065	4.026	363.	*c*	430.7	77.8	122.	411.	98.6
F_2	37.997	3.653	112.	*a*	—	—	—	—	—
Cl_2	70.905	4.115	357.	*a*	417.	76.1	124.	420.	97.0
Br_2	159.808	4.268	520.	*a*	584.	102.	144.	—	—
I_2	253.809	4.982	550.	*a*	800.	—	—	—	—
Hydrocarbons:									
CH_4	16.04	3.780	154.	*b*	191.1	45.8	98.7	159.	158.
CH≡CH	26.04	4.114	212.	*d*	308.7	61.6	112.9	237.	—
CH_2=CH_2	28.05	4.228	216.	*b*	282.4	50.0	124.	215.	—
C_2H_6	30.07	4.388	232.	*b*	305.4	48.2	148.	210.	203.
CH_3C≡CH	40.06	4.742	261.	*d*	394.8	—	—	—	—
CH_3CH=CH_2	42.08	4.766	275.	*b*	365.0	45.5	181.	233.	—
C_3H_8	44.10	4.934	273.	*b*	369.8	41.9	200.	228.	—
n—C_4H_{10}	58.12	5.604	304.	*b*	425.2	37.5	255.	239.	—

n—C_5H_{12}	72.15	5.850	326.	*b*	469.5	33.2	311.	256.	—	
i—C_5H_{12}	72.15	5.812	327.	*b*	460.4	33.7	306.	—	—	
$C(CH_3)_4$	72.15	5.759	312.	*b*	433.8	31.6	303.	—	—	
n—C_6H_{14}	86.18	6.264	342.	*b*	507.3	29.7	370.	248.	—	
n—C_7H_{16}	100.20	6.663	352.	*b*	540.1	27.0	432.	254.	—	
n—C_8H_{18}	114.23	7.035	361.	*b*	568.7	24.5	492	259.	—	
n—C_9H_{20}	128.26	7.463	351.	*b*	594.6	22.6	548.	265.	—	
Cyclohexane	84.16	6.143	313.	*d*	553.	40.0	308.	284.	—	
Benzene	78.11	5.443	387.	*b*	562.6	48.6	260.	312.	—	
Other organic compounds:										
CH_4	16.04	3.780	154.	*b*	191.1	45.8	98.7	159.	158.	
CH_3Cl	50.49	4.151	355.	*c*	416.3	65.9	143.	338.	—	
CH_2Cl_2	84.93	4.748	398.	*c*	510.	60.	—	—	—	
$CHCl_3$	119.38	5.389	340.	*e*	536.6	54.	240.	410.	—	
CCl_4	153.82	5.947	323.	*e*	556.4	45.0	276.	413.	—	
C_2N_2	52.034	4.361	349.	*e*	400.	59.	—	—	—	
COS	60.076	4.130	336.	*e*	378.	61.	—	—	—	
CS_2	76.143	4.483	467.	*e*	552.	78.	170.	404.	—	
CCl_2F_2	120.91	5.116	280.	*b*	384.7	39.6	218.	—	—	

[a] J. O. Hirschfelder, C. F. Curtiss, and R. B. Bird, *Molecular Theory of Gases and Liquids*, corrected printing with notes added, Wiley, New York (1964).

[b] L. S. Tee, S. Gotoh, and W. E. Stewart, *Ind. Eng. Chem. Fundamentals*, **5**, 356–363 (1966). The values for benzene are from viscosity data on that substance. The values for other substances are computed from Correlation (iii) of the paper.

[c] L. Monchick and E. A. Mason, *J. Chem. Phys.*, **35**, 1676–1697 (1961); parameters obtained from viscosity.

[d] L. W. Flynn and G. Thodos, *AIChE Journal*, **8**, 362–365 (1962); parameters obtained from viscosity.

[e] R. A. Svehla, *NASA Tech. Report R-132* (1962); parameters obtained from viscosity. This report provides extensive tables of Lennard-Jones parameters, heat capacities, and calculated transport properties.

[f] Values of the critical constants for the pure substances are selected from K. A. Kobe and R. E. Lynn, Jr., *Chem. Rev.*, **52**, 117–236 (1962); *Amer. Petroleum Inst. Research Proj.* **44**, Thermodynamics Research Center, Texas A&M University, College Station, Texas (1966); and *Thermodynamic Functions of Gases*, F. Din (editor), Vols. 1–3, Butterworths, London (1956, 1961, 1962).

[g] Values of the critical viscosity are from O. A. Hougen and K. M. Watson, *Chemical Process Principles*, Vol. 3, Wiley, New York (1947), p. 873.

[h] Values of the critical thermal conductivity are from E. J. Owens and G. Thodos, *AIChE Journal*, **3**, 454–461 (1957).

[i] For air, the molecular weight M and the pseudocritical properties have been computed from the average composition of dry air as given in COESA, *U.S. Standard Atmosphere 1976*, U.S. Government Printing Office, Washington, D.C. (1976).

Table E.2 Collision Integrals for Use with the Lennard-Jones (6–12) Potential for the Prediction of Transport Properties of Gases at Low Densities[a,b,c]

$\kappa T/\varepsilon$ or $\kappa T/\varepsilon_{AB}$	$\Omega_\mu = \Omega_k$ (for viscosity and thermal conductivity)	$\Omega_{\mathfrak{D},AB}$ (for diffusivity)	$\kappa T/\varepsilon$ or $\kappa T/\varepsilon_{AB}$	$\Omega_\mu = \Omega_k$ (for viscosity and thermal conductivity)	$\Omega_{\mathfrak{D},AB}$ (for diffusivity)
0.30	2.840	2.649	2.7	1.0691	0.9782
0.35	2.676	2.468	2.8	1.0583	0.9682
0.40	2.531	2.314	2.9	1.0482	0.9588
0.45	2.401	2.182	3.0	1.0388	0.9500
0.50	2.284	2.066	3.1	1.0300	0.9418
0.55	2.178	1.965	3.2	1.0217	0.9340
0.60	2.084	1.877	3.3	1.0139	0.9267
0.65	1.999	1.799	3.4	1.0066	0.9197
0.70	1.922	1.729	3.5	0.9996	0.9131
0.75	1.853	1.667	3.6	0.9931	0.9068
0.80	1.790	1.612	3.7	0.9868	0.9008
0.85	1.734	1.562	3.8	0.9809	0.8952
0.90	1.682	1.517	3.9	0.9753	0.8897
0.95	1.636	1.477	4.0	0.9699	0.8845
1.00	1.593	1.440	4.1	0.9647	0.8796
1.05	1.554	1.406	4.2	0.9598	0.8748
1.10	1.518	1.375	4.3	0.9551	0.8703
1.15	1.485	1.347	4.4	0.9506	0.8659
1.20	1.455	1.320	4.5	0.9462	0.8617
1.25	1.427	1.296	4.6	0.9420	0.8576
1.30	1.401	1.274	4.7	0.9380	0.8537
1.35	1.377	1.253	4.8	0.9341	0.8499
1.40	1.355	1.234	4.9	0.9304	0.8463
1.45	1.334	1.216	5.0	0.9268	0.8428
1.50	1.315	1.199	6.0	0.8962	0.8129
1.55	1.297	1.183	7.0	0.8727	0.7898
1.60	1.280	1.168	8.0	0.8538	0.7711
1.65	1.264	1.154	9.0	0.8380	0.7555
1.70	1.249	1.141	10.0	0.8244	0.7422
1.75	1.235	1.128	12.0	0.8018	0.7202
1.80	1.222	1.117	14.0	0.7836	0.7025
1.85	1.209	1.105	16.0	0.7683	0.6878
1.90	1.198	1.095	18.0	0.7552	0.6751
1.95	1.186	1.085	20.0	0.7436	0.6640
2.00	1.176	1.075	25.0	0.7198	0.6414
2.10	1.156	1.058	30.0	0.7010	0.6235
2.20	1.138	1.042	35.0	0.6854	0.6088
2.30	1.122	1.027	40.0	0.6723	0.5964
2.40	1.107	1.013	50.0	0.6510	0.5763
2.50	1.0933	1.0006	75.0	0.6140	0.5415
2.60	1.0807	0.9890	100.0	0.5887	0.5180

[a] The values in this table, applicable for the Lennard-Jones (6–12) potential, are interpolated from the results of L. Monchick and E. A. Mason, *J. Chem. Phys.*, 35, 1676–1697 (1961). The Monchick–Mason table is believed to be slightly better than the earlier table by J. O. Hirschfelder, R. B. Bird, and E. L. Spotz, *J. Chem. Phys.*, 16, 968–981 (1948).

[b] This table has been extended to lower temperatures by C. F. Curtiss, *J. Chem. Phys.*, 97, 7679–7686 (1992). Curtiss showed that at low temperatures, the Boltzmann equation needs to be modified to take into account "orbiting pairs" of molecules. Only by making this modification is it possible to get a smooth transition from quantum to classical behavior. The deviations are appreciable below dimensionless temperatures of 0.30.

[c] The collision integrals have been curve-fitted by P. D. Neufeld, A. R. Jansen, and R. A. Aziz, *J. Chem. Phys.*, 57, 1100–1102 (1972), as follows:

$$\Omega_\mu = \Omega_k = \frac{1.16145}{T^{*0.14874}} + \frac{0.52487}{\exp(0.77320T^*)} + \frac{2.16178}{\exp(2.43787T^*)} \tag{E.2-1}$$

$$\Omega_{\mathfrak{D},AB} = \frac{1.06036}{T^{*0.15610}} + \frac{0.19300}{\exp(0.47635T^*)} + \frac{1.03587}{\exp(1.52996T^*)} + \frac{1.76474}{\exp(3.89411T^*)} \tag{E.2-2}$$

where $T^* = \kappa T/\varepsilon$.

APPENDIX 5

Permeability of pure component across gamma alumina membrane

Effect of pore size

1. Insert the desired pore size range, rp (m)

$i := 1,2..40$

$rp_i := 0.1 \cdot 10^{-9} \cdot i$

2. Input the desired operation temperature (K) and pressure (atm)

$T := 363$

$P := 60$

3. Input the membrane properties:
   ε - porosity, τ - tortuosity, tm - thickness, ρm - density

$\varepsilon := 0.603$

$\tau := 1.658$

$tm := 1 \cdot 10^{-7}$

$\rho m := 3040$

4. Input the properties of the gas components:
   1 - Carbon dioxide, 2 - Methane, 3 - Hydrogen sulfide
   M - Molecular weight (g/mol), Φ - diameter (m), Ω - Lennard-Jones Constant,
   ΔH - Heat of adsorption (J/mol), f - equilibrium loading factor (m3/kg), z - compressibility factor
   Ru - universal gas constant (cm3.atm/mol.K)

$M1 := 44.01$

$M2 := 16.043$

$M3 := 34.04$

$\Phi 1 := 3.3$

$\Phi 2 := 3.88$

$\Omega 1 := 1.2988$

$\Omega 2 := 1.1361$

$\Delta H1 := -17116$

$\Delta H2 := -21000$

$\Delta H3 := -18780$

$f1 := \frac{1}{\rho m}$

$f2 := \frac{1}{\rho m}$

$f3 := \frac{1}{\rho m}$

$Tc1 := 304.1$

$Tc2 := 190.6$

$Tc3 := 373.2$

$Pc1 := 73.8$

$Pc2 := 46$

$Pc3 := 89.4$

$z3 := 0.674$

$z1 := 0.9914$

$z2 := 0.9520$

$Ru := 82.06$

5. Input the viscousity, μ of gas components

$$\mu 1 := 2.6693 \cdot 10^{-5} \cdot \frac{\sqrt{M1 \cdot T}}{\Phi 1^2 \cdot \Omega 1} \cdot \frac{100}{1000}$$

$$\mu 1 = 2.385 \times 10^{-5}$$

$$\mu 2 := 2.6693 \cdot 10^{-5} \cdot \frac{\sqrt{M2 \cdot T}}{\Phi 2^2 \cdot \Omega 2} \cdot \frac{100}{1000}$$

$$\mu 2 = 1.191 \times 10^{-5}$$

$$\mu 3 := 1.7331 \cdot 10^{-5}$$

6. Calculate the permeability (mol.s/kg) of gas components due to viscous diffusion.

$$Pv1_i := \frac{\varepsilon \cdot \left(rp_i\right)^2 \cdot \left(\frac{P + 1.2}{2}\right)}{8 \cdot \tau \cdot \mu 1 \cdot z1 \cdot Ru \cdot T \cdot \left(\frac{1}{10^6}\right)}$$

$$Pv2_i := \frac{\varepsilon \cdot \left(rp_i\right)^2 \cdot \left(\frac{P + 1.2}{2}\right)}{8 \cdot \tau \cdot \mu 2 \cdot z2 \cdot Ru \cdot T \cdot \left(\frac{1}{10^6}\right)}$$

$$Pv3_i := \frac{\varepsilon \cdot \left(rp_i\right)^2 \cdot \left(\frac{P + 1.2}{2}\right)}{8 \cdot \tau \cdot \mu 3 \cdot z3 \cdot Ru \cdot T \cdot \left(\frac{1}{10^6}\right)}$$

rp_i =	$Pv1_i$ =	$Pv2_i$ =	$Pv3_i$ =
$1 \cdot 10^{-10}$	$1.975 \cdot 10^{-14}$	$4.119 \cdot 10^{-14}$	$3.998 \cdot 10^{-14}$
$2 \cdot 10^{-10}$	$7.899 \cdot 10^{-14}$	$1.648 \cdot 10^{-13}$	$1.599 \cdot 10^{-13}$
$3 \cdot 10^{-10}$	$1.777 \cdot 10^{-13}$	$3.707 \cdot 10^{-13}$	$3.598 \cdot 10^{-13}$
$4 \cdot 10^{-10}$	$3.16 \cdot 10^{-13}$	$6.59 \cdot 10^{-13}$	$6.397 \cdot 10^{-13}$
$5 \cdot 10^{-10}$	$4.937 \cdot 10^{-13}$	$1.03 \cdot 10^{-12}$	$9.995 \cdot 10^{-13}$
$6 \cdot 10^{-10}$	$7.109 \cdot 10^{-13}$	$1.483 \cdot 10^{-12}$	$1.439 \cdot 10^{-12}$
$7 \cdot 10^{-10}$	$9.676 \cdot 10^{-13}$	$2.018 \cdot 10^{-12}$	$1.959 \cdot 10^{-12}$
$8 \cdot 10^{-10}$	$1.264 \cdot 10^{-12}$	$2.636 \cdot 10^{-12}$	$2.559 \cdot 10^{-12}$
$9 \cdot 10^{-10}$	$1.6 \cdot 10^{-12}$	$3.336 \cdot 10^{-12}$	$3.238 \cdot 10^{-12}$
$1 \cdot 10^{-9}$	$1.975 \cdot 10^{-12}$	$4.119 \cdot 10^{-12}$	$3.998 \cdot 10^{-12}$
$1.1 \cdot 10^{-9}$	$2.389 \cdot 10^{-12}$	$4.984 \cdot 10^{-12}$	$4.838 \cdot 10^{-12}$
$1.2 \cdot 10^{-9}$	$2.844 \cdot 10^{-12}$	$5.931 \cdot 10^{-12}$	$5.757 \cdot 10^{-12}$
$1.3 \cdot 10^{-9}$	$3.337 \cdot 10^{-12}$	$6.961 \cdot 10^{-12}$	$6.757 \cdot 10^{-12}$
$1.4 \cdot 10^{-9}$	$3.871 \cdot 10^{-12}$	$8.073 \cdot 10^{-12}$	$7.836 \cdot 10^{-12}$
$1.5 \cdot 10^{-9}$	$4.443 \cdot 10^{-12}$	$9.267 \cdot 10^{-12}$	$8.995 \cdot 10^{-12}$
$1.6 \cdot 10^{-9}$	$5.055 \cdot 10^{-12}$	$1.054 \cdot 10^{-11}$	$1.023 \cdot 10^{-11}$
$1.7 \cdot 10^{-9}$	$5.707 \cdot 10^{-12}$	$1.19 \cdot 10^{-11}$	$1.155 \cdot 10^{-11}$
$1.8 \cdot 10^{-9}$	$6.398 \cdot 10^{-12}$	$1.335 \cdot 10^{-11}$	$1.295 \cdot 10^{-11}$
$1.9 \cdot 10^{-9}$	$7.129 \cdot 10^{-12}$	$1.487 \cdot 10^{-11}$	$1.443 \cdot 10^{-11}$
$2 \cdot 10^{-9}$	$7.899 \cdot 10^{-12}$	$1.648 \cdot 10^{-11}$	$1.599 \cdot 10^{-11}$
$2.1 \cdot 10^{-9}$	$8.709 \cdot 10^{-12}$	$1.816 \cdot 10^{-11}$	$1.763 \cdot 10^{-11}$
$2.2 \cdot 10^{-9}$	$9.558 \cdot 10^{-12}$	$1.994 \cdot 10^{-11}$	$1.935 \cdot 10^{-11}$
$2.3 \cdot 10^{-9}$	$1.045 \cdot 10^{-11}$	$2.179 \cdot 10^{-11}$	$2.115 \cdot 10^{-11}$
$2.4 \cdot 10^{-9}$	$1.137 \cdot 10^{-11}$	$2.372 \cdot 10^{-11}$	$2.303 \cdot 10^{-11}$
$2.5 \cdot 10^{-9}$	$1.234 \cdot 10^{-11}$	$2.574 \cdot 10^{-11}$	$2.499 \cdot 10^{-11}$
$2.6 \cdot 10^{-9}$	$1.335 \cdot 10^{-11}$	$2.784 \cdot 10^{-11}$	$2.703 \cdot 10^{-11}$
$2.7 \cdot 10^{-9}$	$1.44 \cdot 10^{-11}$	$3.003 \cdot 10^{-11}$	$2.915 \cdot 10^{-11}$
$2.8 \cdot 10^{-9}$	$1.548 \cdot 10^{-11}$	$3.229 \cdot 10^{-11}$	$3.134 \cdot 10^{-11}$
$2.9 \cdot 10^{-9}$	$1.661 \cdot 10^{-11}$	$3.464 \cdot 10^{-11}$	$3.362 \cdot 10^{-11}$
$3 \cdot 10^{-9}$	$1.777 \cdot 10^{-11}$	$3.707 \cdot 10^{-11}$	$3.598 \cdot 10^{-11}$
$3.1 \cdot 10^{-9}$	$1.898 \cdot 10^{-11}$	$3.958 \cdot 10^{-11}$	$3.842 \cdot 10^{-11}$
$3.2 \cdot 10^{-9}$	$2.022 \cdot 10^{-11}$	$4.218 \cdot 10^{-11}$	$4.094 \cdot 10^{-11}$
$3.3 \cdot 10^{-9}$	$2.151 \cdot 10^{-11}$	$4.485 \cdot 10^{-11}$	$4.354 \cdot 10^{-11}$
$3.4 \cdot 10^{-9}$	$2.283 \cdot 10^{-11}$	$4.761 \cdot 10^{-11}$	$4.622 \cdot 10^{-11}$
$3.5 \cdot 10^{-9}$	$2.419 \cdot 10^{-11}$	$5.046 \cdot 10^{-11}$	$4.898 \cdot 10^{-11}$
$3.6 \cdot 10^{-9}$	$2.559 \cdot 10^{-11}$	$5.338 \cdot 10^{-11}$	$5.181 \cdot 10^{-11}$
$3.7 \cdot 10^{-9}$	$2.703 \cdot 10^{-11}$	$5.639 \cdot 10^{-11}$	$5.473 \cdot 10^{-11}$
$3.8 \cdot 10^{-9}$	$2.852 \cdot 10^{-11}$	$5.948 \cdot 10^{-11}$	$5.773 \cdot 10^{-11}$
$3.9 \cdot 10^{-9}$	$3.004 \cdot 10^{-11}$	$6.265 \cdot 10^{-11}$	$6.081 \cdot 10^{-11}$
$4 \cdot 10^{-9}$	$3.16 \cdot 10^{-11}$	$6.59 \cdot 10^{-11}$	$6.397 \cdot 10^{-11}$

7. Calculate the Knudsen diffusivity (m2/s)

$$Dk1_i := \frac{2}{3}\cdot\left(rp_i - \frac{0.33\cdot10^{-9}}{2}\right)\cdot\sqrt{\frac{8\cdot8.314\cdot1000\cdot T}{3.142\cdot M1}}$$

$$Dk2_i := \frac{2}{3}\cdot\left(rp_i - \frac{0.38\cdot10^{-9}}{2}\right)\cdot\sqrt{\frac{8\cdot8.314\cdot1000\cdot T}{3.142\cdot M2}}$$

$$Dk3_i := \frac{2}{3}\cdot\left(rp_i - \frac{0.36\cdot10^{-9}}{2}\right)\cdot\sqrt{\frac{8\cdot3.14\cdot1000\cdot T}{3.142\cdot M3}}$$

rp_i =	$Dk1_i$ =	$Dk2_i$ =	$Dk3_i$ =
$1\cdot10^{-10}$	$-1.811\cdot10^{-8}$	$-4.152\cdot10^{-8}$	$-1.557\cdot10^{-8}$
$2\cdot10^{-10}$	$9.75\cdot10^{-9}$	$4.614\cdot10^{-9}$	$3.893\cdot10^{-9}$
$3\cdot10^{-10}$	$3.761\cdot10^{-8}$	$5.075\cdot10^{-8}$	$2.336\cdot10^{-8}$
$4\cdot10^{-10}$	$6.546\cdot10^{-8}$	$9.689\cdot10^{-8}$	$4.282\cdot10^{-8}$
$5\cdot10^{-10}$	$9.332\cdot10^{-8}$	$1.43\cdot10^{-7}$	$6.229\cdot10^{-8}$
$6\cdot10^{-10}$	$1.212\cdot10^{-7}$	$1.892\cdot10^{-7}$	$8.176\cdot10^{-8}$
$7\cdot10^{-10}$	$1.49\cdot10^{-7}$	$2.353\cdot10^{-7}$	$1.012\cdot10^{-7}$
$8\cdot10^{-10}$	$1.769\cdot10^{-7}$	$2.814\cdot10^{-7}$	$1.207\cdot10^{-7}$
$9\cdot10^{-10}$	$2.047\cdot10^{-7}$	$3.276\cdot10^{-7}$	$1.402\cdot10^{-7}$
$1\cdot10^{-9}$	$2.326\cdot10^{-7}$	$3.737\cdot10^{-7}$	$1.596\cdot10^{-7}$
$1.1\cdot10^{-9}$	$2.605\cdot10^{-7}$	$4.199\cdot10^{-7}$	$1.791\cdot10^{-7}$
$1.2\cdot10^{-9}$	$2.883\cdot10^{-7}$	$4.66\cdot10^{-7}$	$1.986\cdot10^{-7}$
$1.3\cdot10^{-9}$	$3.162\cdot10^{-7}$	$5.121\cdot10^{-7}$	$2.18\cdot10^{-7}$
$1.4\cdot10^{-9}$	$3.44\cdot10^{-7}$	$5.583\cdot10^{-7}$	$2.375\cdot10^{-7}$
$1.5\cdot10^{-9}$	$3.719\cdot10^{-7}$	$6.044\cdot10^{-7}$	$2.569\cdot10^{-7}$
$1.6\cdot10^{-9}$	$3.997\cdot10^{-7}$	$6.506\cdot10^{-7}$	$2.764\cdot10^{-7}$
$1.7\cdot10^{-9}$	$4.276\cdot10^{-7}$	$6.967\cdot10^{-7}$	$2.959\cdot10^{-7}$
$1.8\cdot10^{-9}$	$4.555\cdot10^{-7}$	$7.428\cdot10^{-7}$	$3.153\cdot10^{-7}$
$1.9\cdot10^{-9}$	$4.833\cdot10^{-7}$	$7.89\cdot10^{-7}$	$3.348\cdot10^{-7}$
$2\cdot10^{-9}$	$5.112\cdot10^{-7}$	$8.351\cdot10^{-7}$	$3.543\cdot10^{-7}$
$2.1\cdot10^{-9}$	$5.39\cdot10^{-7}$	$8.813\cdot10^{-7}$	$3.737\cdot10^{-7}$
$2.2\cdot10^{-9}$	$5.669\cdot10^{-7}$	$9.274\cdot10^{-7}$	$3.932\cdot10^{-7}$
$2.3\cdot10^{-9}$	$5.947\cdot10^{-7}$	$9.735\cdot10^{-7}$	$4.127\cdot10^{-7}$
$2.4\cdot10^{-9}$	$6.226\cdot10^{-7}$	$1.02\cdot10^{-6}$	$4.321\cdot10^{-7}$
$2.5\cdot10^{-9}$	$6.505\cdot10^{-7}$	$1.066\cdot10^{-6}$	$4.516\cdot10^{-7}$
$2.6\cdot10^{-9}$	$6.783\cdot10^{-7}$	$1.112\cdot10^{-6}$	$4.711\cdot10^{-7}$
$2.7\cdot10^{-9}$	$7.062\cdot10^{-7}$	$1.158\cdot10^{-6}$	$4.905\cdot10^{-7}$
$2.8\cdot10^{-9}$	$7.34\cdot10^{-7}$	$1.204\cdot10^{-6}$	$5.1\cdot10^{-7}$
$2.9\cdot10^{-9}$	$7.619\cdot10^{-7}$	$1.25\cdot10^{-6}$	$5.295\cdot10^{-7}$

$3 \cdot 10^{-9}$	$7.897 \cdot 10^{-7}$	$1.296 \cdot 10^{-6}$	$5.489 \cdot 10^{-7}$
$3.1 \cdot 10^{-9}$	$8.176 \cdot 10^{-7}$	$1.343 \cdot 10^{-6}$	$5.684 \cdot 10^{-7}$
$3.2 \cdot 10^{-9}$	$8.455 \cdot 10^{-7}$	$1.389 \cdot 10^{-6}$	$5.879 \cdot 10^{-7}$
$3.3 \cdot 10^{-9}$	$8.733 \cdot 10^{-7}$	$1.435 \cdot 10^{-6}$	$6.073 \cdot 10^{-7}$
$3.4 \cdot 10^{-9}$	$9.012 \cdot 10^{-7}$	$1.481 \cdot 10^{-6}$	$6.268 \cdot 10^{-7}$
$3.5 \cdot 10^{-9}$	$9.29 \cdot 10^{-7}$	$1.527 \cdot 10^{-6}$	$6.463 \cdot 10^{-7}$
$3.6 \cdot 10^{-9}$	$9.569 \cdot 10^{-7}$	$1.573 \cdot 10^{-6}$	$6.657 \cdot 10^{-7}$
$3.7 \cdot 10^{-9}$	$9.847 \cdot 10^{-7}$	$1.619 \cdot 10^{-6}$	$6.852 \cdot 10^{-7}$
$3.8 \cdot 10^{-9}$	$1.013 \cdot 10^{-6}$	$1.666 \cdot 10^{-6}$	$7.047 \cdot 10^{-7}$
$3.9 \cdot 10^{-9}$	$1.04 \cdot 10^{-6}$	$1.712 \cdot 10^{-6}$	$7.241 \cdot 10^{-7}$
$4 \cdot 10^{-9}$	$1.068 \cdot 10^{-6}$	$1.758 \cdot 10^{-6}$	$7.436 \cdot 10^{-7}$

8. Calculate the permeability of gas components (mol.s/kg) due to Knudsen diffusivity

$$Pk1_i := \frac{\varepsilon \cdot \left(\frac{1}{\frac{1}{1.723 \cdot 10^{-5}} + \frac{1}{Dk1_i}} \right)}{z1 \cdot \tau \cdot Ru \cdot T \cdot \left(\frac{101325}{1 \cdot 10^{6}} \right)}$$

$$Pk2_i := \frac{\varepsilon \cdot \left(\frac{1}{\frac{1}{1.723 \cdot 10^{-5}} + \frac{1}{Dk2_i}} \right)}{z2 \cdot \tau \cdot Ru \cdot T \cdot \left(\frac{101325}{1 \cdot 10^{6}} \right)}$$

$$Pk3_i := \frac{\varepsilon \cdot \left(\frac{1}{\frac{1}{1.723 \cdot 10^{-5}} + \frac{1}{Dk3_i}} \right)}{z3 \cdot \tau \cdot Ru \cdot T \cdot \left(\frac{101325}{1 \cdot 10^{6}} \right)}$$

rp_i =	$Pk1_i$ =	$Pk2_i$ =	$Pk3_i$ =
$1 \cdot 10^{-10}$	$-2.203 \cdot 10^{-12}$	$-5.269 \cdot 10^{-12}$	$-2.787 \cdot 10^{-12}$
$2 \cdot 10^{-10}$	$1.184 \cdot 10^{-12}$	$5.838 \cdot 10^{-13}$	$6.959 \cdot 10^{-13}$
$3 \cdot 10^{-10}$	$4.561 \cdot 10^{-12}$	$6.405 \cdot 10^{-12}$	$4.17 \cdot 10^{-12}$
$4 \cdot 10^{-10}$	$7.927 \cdot 10^{-12}$	$1.22 \cdot 10^{-11}$	$7.637 \cdot 10^{-12}$
$5 \cdot 10^{-10}$	$1.128 \cdot 10^{-11}$	$1.795 \cdot 10^{-11}$	$1.11 \cdot 10^{-11}$
$6 \cdot 10^{-10}$	$1.463 \cdot 10^{-11}$	$2.368 \cdot 10^{-11}$	$1.455 \cdot 10^{-11}$
$7 \cdot 10^{-10}$	$1.796 \cdot 10^{-11}$	$2.938 \cdot 10^{-11}$	$1.799 \cdot 10^{-11}$
$8 \cdot 10^{-10}$	$2.128 \cdot 10^{-11}$	$3.505 \cdot 10^{-11}$	$2.143 \cdot 10^{-11}$
$9 \cdot 10^{-10}$	$2.459 \cdot 10^{-11}$	$4.069 \cdot 10^{-11}$	$2.485 \cdot 10^{-11}$
$1 \cdot 10^{-9}$	$2.789 \cdot 10^{-11}$	$4.63 \cdot 10^{-11}$	$2.827 \cdot 10^{-11}$
$1.1 \cdot 10^{-9}$	$3.119 \cdot 10^{-11}$	$5.188 \cdot 10^{-11}$	$3.169 \cdot 10^{-11}$
$1.2 \cdot 10^{-9}$	$3.447 \cdot 10^{-11}$	$5.743 \cdot 10^{-11}$	$3.509 \cdot 10^{-11}$
$1.3 \cdot 10^{-9}$	$3.774 \cdot 10^{-11}$	$6.295 \cdot 10^{-11}$	$3.849 \cdot 10^{-11}$
$1.4 \cdot 10^{-9}$	$4.1 \cdot 10^{-11}$	$6.845 \cdot 10^{-11}$	$4.188 \cdot 10^{-11}$
$1.5 \cdot 10^{-9}$	$4.425 \cdot 10^{-11}$	$7.391 \cdot 10^{-11}$	$4.526 \cdot 10^{-11}$
$1.6 \cdot 10^{-9}$	$4.748 \cdot 10^{-11}$	$7.935 \cdot 10^{-11}$	$4.864 \cdot 10^{-11}$
$1.7 \cdot 10^{-9}$	$5.071 \cdot 10^{-11}$	$8.476 \cdot 10^{-11}$	$5.2 \cdot 10^{-11}$
$1.8 \cdot 10^{-9}$	$5.393 \cdot 10^{-11}$	$9.014 \cdot 10^{-11}$	$5.536 \cdot 10^{-11}$
$1.9 \cdot 10^{-9}$	$5.714 \cdot 10^{-11}$	$9.549 \cdot 10^{-11}$	$5.872 \cdot 10^{-11}$
$2 \cdot 10^{-9}$	$6.034 \cdot 10^{-11}$	$1.008 \cdot 10^{-10}$	$6.206 \cdot 10^{-11}$
$2.1 \cdot 10^{-9}$	$6.353 \cdot 10^{-11}$	$1.061 \cdot 10^{-10}$	$6.54 \cdot 10^{-11}$
$2.2 \cdot 10^{-9}$	$6.671 \cdot 10^{-11}$	$1.114 \cdot 10^{-10}$	$6.873 \cdot 10^{-11}$
$2.3 \cdot 10^{-9}$	$6.988 \cdot 10^{-11}$	$1.166 \cdot 10^{-10}$	$7.205 \cdot 10^{-11}$
$2.4 \cdot 10^{-9}$	$7.303 \cdot 10^{-11}$	$1.219 \cdot 10^{-10}$	$7.537 \cdot 10^{-11}$
$2.5 \cdot 10^{-9}$	$7.618 \cdot 10^{-11}$	$1.27 \cdot 10^{-10}$	$7.868 \cdot 10^{-11}$
$2.6 \cdot 10^{-9}$	$7.932 \cdot 10^{-11}$	$1.322 \cdot 10^{-10}$	$8.198 \cdot 10^{-11}$
$2.7 \cdot 10^{-9}$	$8.245 \cdot 10^{-11}$	$1.374 \cdot 10^{-10}$	$8.527 \cdot 10^{-11}$
$2.8 \cdot 10^{-9}$	$8.557 \cdot 10^{-11}$	$1.425 \cdot 10^{-10}$	$8.856 \cdot 10^{-11}$
$2.9 \cdot 10^{-9}$	$8.868 \cdot 10^{-11}$	$1.476 \cdot 10^{-10}$	$9.184 \cdot 10^{-11}$
$3 \cdot 10^{-9}$	$9.178 \cdot 10^{-11}$	$1.526 \cdot 10^{-10}$	$9.511 \cdot 10^{-11}$
$3.1 \cdot 10^{-9}$	$9.487 \cdot 10^{-11}$	$1.577 \cdot 10^{-10}$	$9.837 \cdot 10^{-11}$
$3.2 \cdot 10^{-9}$	$9.795 \cdot 10^{-11}$	$1.627 \cdot 10^{-10}$	$1.016 \cdot 10^{-10}$
$3.3 \cdot 10^{-9}$	$1.01 \cdot 10^{-10}$	$1.677 \cdot 10^{-10}$	$1.049 \cdot 10^{-10}$
$3.4 \cdot 10^{-9}$	$1.041 \cdot 10^{-10}$	$1.726 \cdot 10^{-10}$	$1.081 \cdot 10^{-10}$
$3.5 \cdot 10^{-9}$	$1.071 \cdot 10^{-10}$	$1.776 \cdot 10^{-10}$	$1.114 \cdot 10^{-10}$
$3.6 \cdot 10^{-9}$	$1.102 \cdot 10^{-10}$	$1.825 \cdot 10^{-10}$	$1.146 \cdot 10^{-10}$
$3.7 \cdot 10^{-9}$	$1.132 \cdot 10^{-10}$	$1.874 \cdot 10^{-10}$	$1.178 \cdot 10^{-10}$
$3.8 \cdot 10^{-9}$	$1.162 \cdot 10^{-10}$	$1.922 \cdot 10^{-10}$	$1.21 \cdot 10^{-10}$
$3.9 \cdot 10^{-9}$	$1.193 \cdot 10^{-10}$	$1.971 \cdot 10^{-10}$	$1.242 \cdot 10^{-10}$
$4 \cdot 10^{-9}$	$1.223 \cdot 10^{-10}$	$2.019 \cdot 10^{-10}$	$1.274 \cdot 10^{-10}$

9. Calculate the surface diffusivity (m2/s)

$$Ds1 := \frac{1.62 \cdot 10^{-2}}{1 \cdot 10^{4}} \cdot 2.712^{\frac{(-0.45) \cdot (-\Delta H1)}{8.314 \cdot T}}$$

$$Ds2 := \frac{1.62 \cdot 10^{-2}}{1 \cdot 10^{4}} \cdot 2.712^{\frac{(-0.45) \cdot (-\Delta H2)}{8.314 \cdot T}}$$

$$Ds3 := \frac{1.62 \cdot 10^{-2}}{1 \cdot 10^{4}} \cdot 2.712^{\frac{(-0.45) \cdot (-\Delta H3)}{8.314 \cdot T}}$$

$$Ds1 = 1.27 \times 10^{-7}$$

$$Ds2 = 7.125 \times 10^{-8}$$

$$Ds3 = 9.913 \times 10^{-8}$$

10. Calculate the permeability of gas components (mol.s/kg) due to surface diffusivity.

$$Ps1_i := \frac{2 \cdot \varepsilon^2 \cdot tm \cdot (1 - \varepsilon) \cdot Ds1 \cdot \rho m \cdot f1}{z1 \cdot \tau^2 \cdot Ru \cdot T \cdot rp_i \cdot \left(\frac{101325}{1 \cdot 10^6}\right)}$$

$$Ps2_i := \frac{2 \cdot \varepsilon^2 \cdot tm \cdot (1 - \varepsilon) \cdot Ds2 \cdot \rho m \cdot f2}{z2 \cdot \tau^2 \cdot Ru \cdot T \cdot rp_i \cdot \left(\frac{101325}{1 \cdot 10^6}\right)}$$

$$Ps3_i := \frac{2 \cdot \varepsilon^2 \cdot tm \cdot (1 - \varepsilon) \cdot Ds3 \cdot \rho m \cdot f3}{z3 \cdot \tau^2 \cdot Ru \cdot T \cdot rp_i \cdot \left(\frac{101325}{1 \cdot 10^6}\right)}$$

rp_i =	$Ps1_i$ =	$Ps2_i$ =	$Ps3_i$ =
$1 \cdot 10^{-10}$	$4.457 \cdot 10^{-9}$	$2.604 \cdot 10^{-9}$	$5.118 \cdot 10^{-9}$
$2 \cdot 10^{-10}$	$2.228 \cdot 10^{-9}$	$1.302 \cdot 10^{-9}$	$2.559 \cdot 10^{-9}$
$3 \cdot 10^{-10}$	$1.486 \cdot 10^{-9}$	$8.681 \cdot 10^{-10}$	$1.706 \cdot 10^{-9}$
$4 \cdot 10^{-10}$	$1.114 \cdot 10^{-9}$	$6.511 \cdot 10^{-10}$	$1.279 \cdot 10^{-9}$
$5 \cdot 10^{-10}$	$8.913 \cdot 10^{-10}$	$5.208 \cdot 10^{-10}$	$1.024 \cdot 10^{-9}$
$6 \cdot 10^{-10}$	$7.428 \cdot 10^{-10}$	$4.34 \cdot 10^{-10}$	$8.53 \cdot 10^{-10}$
$7 \cdot 10^{-10}$	$6.366 \cdot 10^{-10}$	$3.72 \cdot 10^{-10}$	$7.311 \cdot 10^{-10}$
$8 \cdot 10^{-10}$	$5.571 \cdot 10^{-10}$	$3.255 \cdot 10^{-10}$	$6.397 \cdot 10^{-10}$
$9 \cdot 10^{-10}$	$4.952 \cdot 10^{-10}$	$2.894 \cdot 10^{-10}$	$5.686 \cdot 10^{-10}$
$1 \cdot 10^{-9}$	$4.457 \cdot 10^{-10}$	$2.604 \cdot 10^{-10}$	$5.118 \cdot 10^{-10}$
$1.1 \cdot 10^{-9}$	$4.051 \cdot 10^{-10}$	$2.367 \cdot 10^{-10}$	$4.653 \cdot 10^{-10}$
$1.2 \cdot 10^{-9}$	$3.714 \cdot 10^{-10}$	$2.17 \cdot 10^{-10}$	$4.265 \cdot 10^{-10}$
$1.3 \cdot 10^{-9}$	$3.428 \cdot 10^{-10}$	$2.003 \cdot 10^{-10}$	$3.937 \cdot 10^{-10}$
$1.4 \cdot 10^{-9}$	$3.183 \cdot 10^{-10}$	$1.86 \cdot 10^{-10}$	$3.656 \cdot 10^{-10}$
$1.5 \cdot 10^{-9}$	$2.971 \cdot 10^{-10}$	$1.736 \cdot 10^{-10}$	$3.412 \cdot 10^{-10}$
$1.6 \cdot 10^{-9}$	$2.785 \cdot 10^{-10}$	$1.628 \cdot 10^{-10}$	$3.199 \cdot 10^{-10}$
$1.7 \cdot 10^{-9}$	$2.621 \cdot 10^{-10}$	$1.532 \cdot 10^{-10}$	$3.01 \cdot 10^{-10}$
$1.8 \cdot 10^{-9}$	$2.476 \cdot 10^{-10}$	$1.447 \cdot 10^{-10}$	$2.843 \cdot 10^{-10}$
$1.9 \cdot 10^{-9}$	$2.346 \cdot 10^{-10}$	$1.371 \cdot 10^{-10}$	$2.694 \cdot 10^{-10}$
$2 \cdot 10^{-9}$	$2.228 \cdot 10^{-10}$	$1.302 \cdot 10^{-10}$	$2.559 \cdot 10^{-10}$
$2.1 \cdot 10^{-9}$	$2.122 \cdot 10^{-10}$	$1.24 \cdot 10^{-10}$	$2.437 \cdot 10^{-10}$
$2.2 \cdot 10^{-9}$	$2.026 \cdot 10^{-10}$	$1.184 \cdot 10^{-10}$	$2.326 \cdot 10^{-10}$
$2.3 \cdot 10^{-9}$	$1.938 \cdot 10^{-10}$	$1.132 \cdot 10^{-10}$	$2.225 \cdot 10^{-10}$
$2.4 \cdot 10^{-9}$	$1.857 \cdot 10^{-10}$	$1.085 \cdot 10^{-10}$	$2.132 \cdot 10^{-10}$
$2.5 \cdot 10^{-9}$	$1.783 \cdot 10^{-10}$	$1.042 \cdot 10^{-10}$	$2.047 \cdot 10^{-10}$
$2.6 \cdot 10^{-9}$	$1.714 \cdot 10^{-10}$	$1.002 \cdot 10^{-10}$	$1.968 \cdot 10^{-10}$
$2.7 \cdot 10^{-9}$	$1.651 \cdot 10^{-10}$	$9.645 \cdot 10^{-11}$	$1.895 \cdot 10^{-10}$
$2.8 \cdot 10^{-9}$	$1.592 \cdot 10^{-10}$	$9.301 \cdot 10^{-11}$	$1.828 \cdot 10^{-10}$
$2.9 \cdot 10^{-9}$	$1.537 \cdot 10^{-10}$	$8.98 \cdot 10^{-11}$	$1.765 \cdot 10^{-10}$
$3 \cdot 10^{-9}$	$1.486 \cdot 10^{-10}$	$8.681 \cdot 10^{-11}$	$1.706 \cdot 10^{-10}$
$3.1 \cdot 10^{-9}$	$1.438 \cdot 10^{-10}$	$8.401 \cdot 10^{-11}$	$1.651 \cdot 10^{-10}$
$3.2 \cdot 10^{-9}$	$1.393 \cdot 10^{-10}$	$8.138 \cdot 10^{-11}$	$1.599 \cdot 10^{-10}$
$3.3 \cdot 10^{-9}$	$1.35 \cdot 10^{-10}$	$7.892 \cdot 10^{-11}$	$1.551 \cdot 10^{-10}$
$3.4 \cdot 10^{-9}$	$1.311 \cdot 10^{-10}$	$7.659 \cdot 10^{-11}$	$1.505 \cdot 10^{-10}$
$3.5 \cdot 10^{-9}$	$1.273 \cdot 10^{-10}$	$7.441 \cdot 10^{-11}$	$1.462 \cdot 10^{-10}$
$3.6 \cdot 10^{-9}$	$1.238 \cdot 10^{-10}$	$7.234 \cdot 10^{-11}$	$1.422 \cdot 10^{-10}$
$3.7 \cdot 10^{-9}$	$1.204 \cdot 10^{-10}$	$7.038 \cdot 10^{-11}$	$1.383 \cdot 10^{-10}$
$3.8 \cdot 10^{-9}$	$1.173 \cdot 10^{-10}$	$6.853 \cdot 10^{-11}$	$1.347 \cdot 10^{-10}$
$3.9 \cdot 10^{-9}$	$1.143 \cdot 10^{-10}$	$6.678 \cdot 10^{-11}$	$1.312 \cdot 10^{-10}$
$4 \cdot 10^{-9}$	$1.114 \cdot 10^{-10}$	$6.511 \cdot 10^{-11}$	$1.279 \cdot 10^{-10}$

11. Calculate the total permeability of gas components (mol.s/kg).

$$Pt1_i := Pv1_i + Pk1_i + Ps1_i$$

$$Pt2_i := Pv2_i + Pk2_i + Ps2_i$$

$$Pt3_i := Pv3_i + Pk3_i + Ps3_i$$

$rp_i =$	$Pt1_i =$	$Pt2_i =$	$Pt3_i =$
$1 \cdot 10^{-10}$	$4.454 \cdot 10^{-9}$	$2.599 \cdot 10^{-9}$	$5.115 \cdot 10^{-9}$
$2 \cdot 10^{-10}$	$2.23 \cdot 10^{-9}$	$1.303 \cdot 10^{-9}$	$2.56 \cdot 10^{-9}$
$3 \cdot 10^{-10}$	$1.49 \cdot 10^{-9}$	$8.749 \cdot 10^{-10}$	$1.71 \cdot 10^{-9}$
$4 \cdot 10^{-10}$	$1.122 \cdot 10^{-9}$	$6.639 \cdot 10^{-10}$	$1.288 \cdot 10^{-9}$
$5 \cdot 10^{-10}$	$9.031 \cdot 10^{-10}$	$5.398 \cdot 10^{-10}$	$1.036 \cdot 10^{-9}$
$6 \cdot 10^{-10}$	$7.581 \cdot 10^{-10}$	$4.592 \cdot 10^{-10}$	$8.69 \cdot 10^{-10}$
$7 \cdot 10^{-10}$	$6.556 \cdot 10^{-10}$	$4.034 \cdot 10^{-10}$	$7.511 \cdot 10^{-10}$
$8 \cdot 10^{-10}$	$5.796 \cdot 10^{-10}$	$3.632 \cdot 10^{-10}$	$6.637 \cdot 10^{-10}$
$9 \cdot 10^{-10}$	$5.214 \cdot 10^{-10}$	$3.334 \cdot 10^{-10}$	$5.967 \cdot 10^{-10}$
$1 \cdot 10^{-9}$	$4.755 \cdot 10^{-10}$	$3.108 \cdot 10^{-10}$	$5.441 \cdot 10^{-10}$
$1.1 \cdot 10^{-9}$	$4.387 \cdot 10^{-10}$	$2.936 \cdot 10^{-10}$	$5.018 \cdot 10^{-10}$
$1.2 \cdot 10^{-9}$	$4.087 \cdot 10^{-10}$	$2.804 \cdot 10^{-10}$	$4.673 \cdot 10^{-10}$
$1.3 \cdot 10^{-9}$	$3.839 \cdot 10^{-10}$	$2.702 \cdot 10^{-10}$	$4.389 \cdot 10^{-10}$
$1.4 \cdot 10^{-9}$	$3.632 \cdot 10^{-10}$	$2.625 \cdot 10^{-10}$	$4.153 \cdot 10^{-10}$
$1.5 \cdot 10^{-9}$	$3.458 \cdot 10^{-10}$	$2.568 \cdot 10^{-10}$	$3.954 \cdot 10^{-10}$
$1.6 \cdot 10^{-9}$	$3.311 \cdot 10^{-10}$	$2.527 \cdot 10^{-10}$	$3.787 \cdot 10^{-10}$
$1.7 \cdot 10^{-9}$	$3.186 \cdot 10^{-10}$	$2.498 \cdot 10^{-10}$	$3.646 \cdot 10^{-10}$
$1.8 \cdot 10^{-9}$	$3.079 \cdot 10^{-10}$	$2.482 \cdot 10^{-10}$	$3.526 \cdot 10^{-10}$
$1.9 \cdot 10^{-9}$	$2.988 \cdot 10^{-10}$	$2.474 \cdot 10^{-10}$	$3.425 \cdot 10^{-10}$
$2 \cdot 10^{-9}$	$2.911 \cdot 10^{-10}$	$2.475 \cdot 10^{-10}$	$3.339 \cdot 10^{-10}$
$2.1 \cdot 10^{-9}$	$2.845 \cdot 10^{-10}$	$2.483 \cdot 10^{-10}$	$3.267 \cdot 10^{-10}$
$2.2 \cdot 10^{-9}$	$2.788 \cdot 10^{-10}$	$2.497 \cdot 10^{-10}$	$3.207 \cdot 10^{-10}$
$2.3 \cdot 10^{-9}$	$2.741 \cdot 10^{-10}$	$2.516 \cdot 10^{-10}$	$3.157 \cdot 10^{-10}$
$2.4 \cdot 10^{-9}$	$2.701 \cdot 10^{-10}$	$2.541 \cdot 10^{-10}$	$3.116 \cdot 10^{-10}$
$2.5 \cdot 10^{-9}$	$2.668 \cdot 10^{-10}$	$2.57 \cdot 10^{-10}$	$3.084 \cdot 10^{-10}$
$2.6 \cdot 10^{-9}$	$2.641 \cdot 10^{-10}$	$2.602 \cdot 10^{-10}$	$3.058 \cdot 10^{-10}$
$2.7 \cdot 10^{-9}$	$2.619 \cdot 10^{-10}$	$2.638 \cdot 10^{-10}$	$3.04 \cdot 10^{-10}$
$2.8 \cdot 10^{-9}$	$2.602 \cdot 10^{-10}$	$2.678 \cdot 10^{-10}$	$3.027 \cdot 10^{-10}$
$2.9 \cdot 10^{-9}$	$2.59 \cdot 10^{-10}$	$2.72 \cdot 10^{-10}$	$3.019 \cdot 10^{-10}$
$3 \cdot 10^{-9}$	$2.581 \cdot 10^{-10}$	$2.765 \cdot 10^{-10}$	$3.017 \cdot 10^{-10}$
$3.1 \cdot 10^{-9}$	$2.576 \cdot 10^{-10}$	$2.812 \cdot 10^{-10}$	$3.019 \cdot 10^{-10}$

$3.2 \cdot 10^{-9}$	$2.574 \cdot 10^{-10}$	$2.862 \cdot 10^{-10}$	$3.025 \cdot 10^{-10}$
$3.3 \cdot 10^{-9}$	$2.576 \cdot 10^{-10}$	$2.914 \cdot 10^{-10}$	$3.035 \cdot 10^{-10}$
$3.4 \cdot 10^{-9}$	$2.58 \cdot 10^{-10}$	$2.968 \cdot 10^{-10}$	$3.049 \cdot 10^{-10}$
$3.5 \cdot 10^{-9}$	$2.587 \cdot 10^{-10}$	$3.024 \cdot 10^{-10}$	$3.066 \cdot 10^{-10}$
$3.6 \cdot 10^{-9}$	$2.596 \cdot 10^{-10}$	$3.082 \cdot 10^{-10}$	$3.086 \cdot 10^{-10}$
$3.7 \cdot 10^{-9}$	$2.607 \cdot 10^{-10}$	$3.141 \cdot 10^{-10}$	$3.109 \cdot 10^{-10}$
$3.8 \cdot 10^{-9}$	$2.62 \cdot 10^{-10}$	$3.202 \cdot 10^{-10}$	$3.134 \cdot 10^{-10}$
$3.9 \cdot 10^{-9}$	$2.636 \cdot 10^{-10}$	$3.265 \cdot 10^{-10}$	$3.163 \cdot 10^{-10}$
$4 \cdot 10^{-9}$	$2.653 \cdot 10^{-10}$	$3.329 \cdot 10^{-10}$	$3.194 \cdot 10^{-10}$

12. Plot the graphs of permeability due to each diffusivity and total permeability against the pore size for every gas components.

*Plotted in Microsoft Excel